Lepton identification in proton-proton collisions with trilepton final state model using Machine Learning?

Kristoffer Langstad

Thesis submitted for the degree of
Master in Computational Science: Physics
60 credits

Department of Physics
Faculty of mathematics and natural sciences

UNIVERSITY OF OSLO

Spring 2021

Lepton identification in proton-proton collisions with trilepton final state model using Machine Learning?

Kristoffer Langstad

Lepton identification in proton-proton collisions with trilepton final state model using Machine Learning?

http://www.duo.uio.no/

Printed: Reprosentralen, University of Oslo

Abstract

...

Acknowledgements

Contents

Introduction

- Standard introduction theory/background:... (mention dark matter?)
- Short explanation of what the chapters contain:...

Notation and Conventions

- $e = 1.6 \cdot 10^{-19}$ C : The elementary charge.
- $c = 2.998 \times 10^8$ m/s: Speed of light in vacuum.
- 1 GeV $= 10^9$ eV $= 10^9 \times 1.602 \times 10^{-19}$ J: Approximately the rest mass energy of the proton.
- $m_e = 9.109 \times 10^{-31}$ kg $= 0.511$ MeV/c^2: Mass of an electron.
- 1 barn (b) $\equiv 10^{-28}$ m^2: Interaction cross sections (dimension of area).
- $h = 6.626 \times 10^{-34}$ J·s: Planck's constant, a fundamental physical constant.
- $\hbar = \frac{h}{2\pi} = 1.055 \times 10^{-34}$ J·s: Unit of action in quantum mechanics (also called the reduced Planck constant).
- Einstein energy-momentum formula: $E^2 = p^2c^2 + m_o^2c^4$
- Coulomb force between two charged particles: $F = \frac{q_1q_2}{4\pi\epsilon_0 r^2}$
- Natural units (from S.I. units):
  - Replace [kg, m, s] with [$\hbar$, c, GeV].
  - $\hbar c = 197$ MeV fm.
  - Use $\hbar = c = \epsilon_0 = \mu_0 = 1$.
- 1D time-dependent Schrödinger equation:

$$i\frac{\partial\psi(\mathbf{x},t)}{\partial t} = -\frac{1}{2m}\frac{\partial^2\psi(\mathbf{x},t)}{\partial x^2} + \hat{V}\psi(\mathbf{x},t)$$

- Planck scale $\sim 10^{19}$ GeV.
- GUT scale $\sim 10^{16}$ GeV.
- Magnetic fields are measured in Tesla (T).

Chapter 1

The Standard Model of Particle Physics

Throughout the years, there have been many theories in physics of what the universe is made up of and how everything fits together. For now, the best theory/model is the Standard Model of particle physics. This theory has many times through the years proven to successfully predict and explain particles and their interactions. This model has lead to what we call elementary particles and fundamental forces, and they are the building blocks of the universe.

In this chapter we look closer at the contents of the Standard Model involving the particles and forces, and going deeper into other underlying theories and models. Much of the information in this chapter is based upon Thomson [1] and some Elert [2].

1.1 Particle and Force Contents

The known elementary particles can be categorized into two main categories according to their spins; fermions and bosons. Fermions have half-integer spins, while bosons have integer spins. The Higgs boson is categorized as a boson but has 0 spin. In Figure 1.1 we see the categorization of the elementary particles, and the fundamental forces, in the Standard Model. The individual categorizations will be explained in the upcoming sections. The interactions in the Standard Model between the particles can be seen in Figure 1.2.

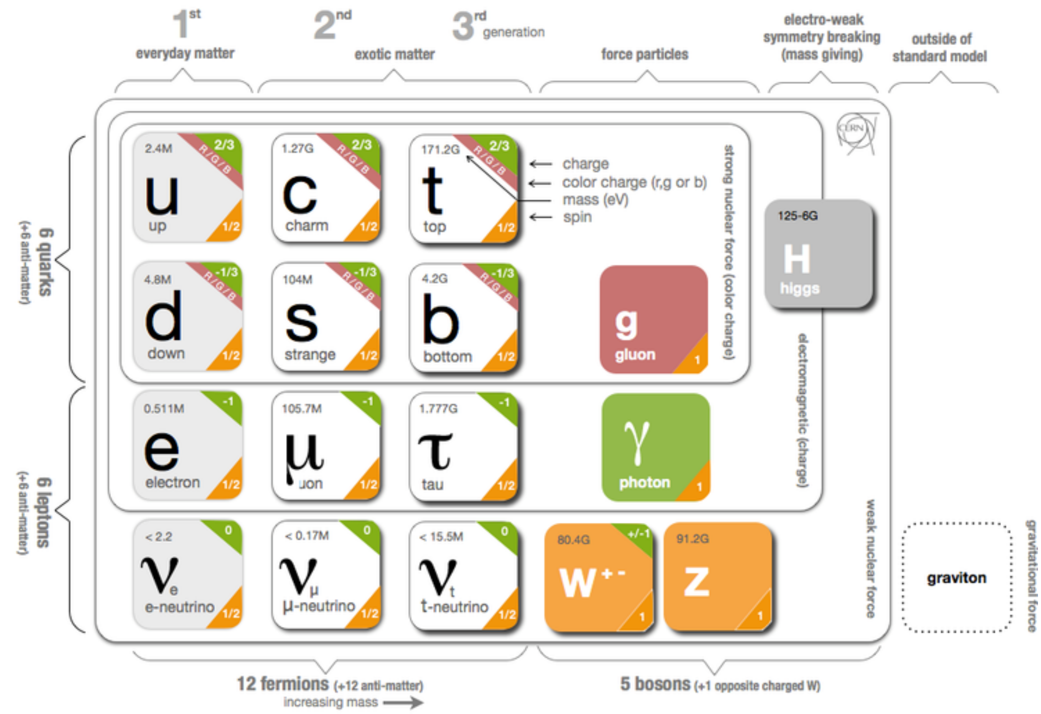

Figure 1.1: The Standard Model contents, source [3].

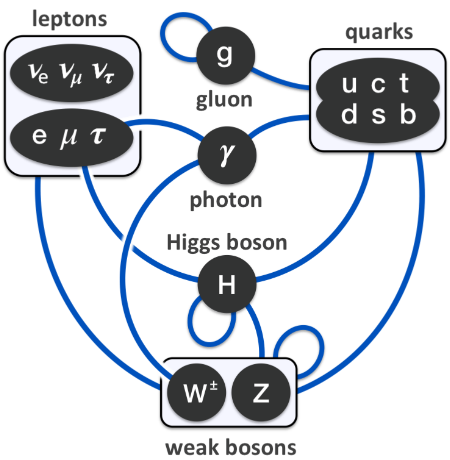

Figure 1.2: The interaction between the particles in the Standard Model. Credit: Wikipedia.

1.1.1 Gauge Bosons

From what we know of, there exists four fundamental forces. Three of these can be explained by the Standard Model through interaction of (gauge) bosons. That is why bosons also are called force-carrier particles. The three forces are the electromagnetic, strong and weak nuclear forces, where each force has its own connected boson(s). There are five different bosons that mediates these forces, and they all have integer spins. This means that they go with vector fields, along a direction.

Strong nuclear force

The strong nuclear force is mediated by eight massless gluon (g) bosons. They only affect the (r,g,b) color charged quarks, and come in combinations of color and anti-color charges. Since the six gluons carry a different variation of color and anti-color combinations, they come in an octet of colored states. The color assignments of these eight physical gluon variations can be written as:

$$b\bar{g}, b\bar{r}, g\bar{b}, g\bar{r}, r\bar{b}, r\bar{g}, \frac{1}{\sqrt{2}}(r\bar{r} - g\bar{g}), \frac{1}{\sqrt{6}}(r\bar{r} + g\bar{g} - 2b\bar{b})$$

It is this strong interaction force that binds the quarks together to make protons and neutrons. The gluons can also self-interact with each other. This makes the interaction range of the strong nuclear force short, keeping the gluons within the nucleus. The exchange of gluons by interactions of colored particles is a mathematical model known as quantum chromodynamics (QCD, sect.1.4.2).

Electromagnetic force

The electromagnetic force is mediated by the massless photon (γ). Photons have an effect on the electrically charged particles. Since the photon is also stable and electrically neutral, it has an infinite range. The electromagnetic force is responsible for holding electrons in place around an atom, and is not as strong as the strong nuclear force. The electrically charged particles are either attracted to each other or repelled away for each other, dependent on if the charges of the particles have the same sign or not. The exchange of photons by interactions of charged particles is a mathematical model known as quantum electrodynamics (QED, sect.1.4.2).

Weak nuclear force

The weak nuclear force is mediated by the $W^{\pm}$ and Z^0 bosons. They have an affect on the flavor of the particles. There are two charge variants of the W charged boson that is either $+e$ or $-e$. The Z boson is electrically neutral. They er both massive compared to many of the other elementary particles, which gives a short lifetime and short range. Because of the difference in their charges, they act on various particles. The W boson couples the electromagnetic interactions, and also act on only left-handed particles and right-handed antiparticles. The W boson can decay to all flavors of quarks, except the top quark which is too massive, to three possible leptonic final states or hadronic final states. The Z boson interacts with left-handed particles and antiparticles. This weak interaction force can also change the flavor of quarks, and also covers isospin. The exchange of W and Z bosons by interactions with flavored particles is explained with a more complex mathematical model that unifies both the weak and electromagnetic interactions, and it is known as electroweak theory (EWT, sect.1.4.2).

Gravitational force

The last force of nature is gravity. We have not yet found the hypothetical graviton (G) particle which should carry the gravitational force. All the other forces seem to be well explained in the Standard Model, except for gravity. So the gravitational force is not included in the Standard Model. There has been a lot of theories about the graviton and a lot of experiments. LIGO and Virgo discovered in 2015 gravitational waves from observing the merging of two black holes with ∼30 solar masses each [4], which might give insight into gravitons. So far, we have nothing conclusive if the graviton exists, yet. It is thought that the graviton would have spin two, since the gravitational waves is described in general relativity as a propagating tensor disturbance. When looking at small objects (micro size), gravity does not seem to have any noticeable effect. But when we look at bigger objects of mass like humans or planets (macro size), then gravity has a much bigger effect and is well described by Einstein's General Theory of Relativity. Since gravity has more or less a negligible effect on particles, particle physicists does not have to take gravity into consideration.

1.1.2 Higgs Boson

The Higgs boson is a "recently" discovered particle (2012) [5][6] theorized by Peter Higgs in 1964. This particle has intrinsic no spin, which makes it a scalar particle, and the only scalar particle discovered so far. Its electrically neutral, and it's massive ($m_H \approx$125 GeV) such that it interacts with itself. Since it is so massive, the lifetime of the Higgs boson is very short and it's hard to detect. It can in principle also decay to all Standard Model particles, but it seems to favor the heavier particles more.

The discovery of the Higgs boson was a big contribution to the Standard Model since it unifies and explains the masses of the other elementary particles, and why the gluons and the photon have no mass. It also confirmed the existence of the Higgs (scalar) field, which gives the other elementary particles mass when they interact with this field. This field is thought to be everywhere in the universe with a non-zero vacuum expectation value. Here, Higgs bosons appear and disappear and interact with other particles in the field giving them their masses. The gluons and photons does not interact with this field, hence they are massless.

1.1.3 Fermions

The fermion group in the Standard Model consists of 12 elementary particles with half-integer spins. These particles are also known as matter-particles, since these particles are the building blocks of the universe. Because of their half-spins, no more than one fermion can occupy a given quantum state for a given quantum number. This is called the Pauli exclusion principle [7] which all fermions obey. Each fermion also has its own antiparticle. The antiparticles have the same mass as their particle partner, but has opposite charges and different quantum numbers. Particles that acts as their own antiparticles are called Majorana particles.

The 12 fermions can be split into two groups of six in quarks and leptons, according to how they interact from their charges. The fermions can then be related into pairs of generations, which goes from lighter and more stable to heavier and less stable. As seen in the SM figure (1.1), the first generation is called the "everyday matter". This is because most of the stable (baryonic) matter is made from the more stable first generation particles. The reason for this is that the first generation particles do not decay. second and third generation particles are more observed in high-energy environments. None of the neutrinos decay, but they rarely interact with baryonic matter.

Quarks

The six quarks are up, down, charm, strange, top and bottom. A characteristic property for the quarks is that they all have color charges and electric charges, affected by the gluons and strong nuclear force. They also carry weak isospin The colors come in red, green and blue and the all have an anti-color. Quarks cannot come as free particles, except for the top quark which is the heaviest elementary particle. This leads to a strong binding between quarks as seen in the description of the strong nuclear force (sect.1.1.1). From this strong binding force, the quarks form particles called hadrons like protons and neutrons. They are made up of either three quarks (baryons/triplets) or a quark and an anti-quark (mesons/doublets). A proton is made up of one down quark and two up quarks. The hadrons are color-neutral particles. Since quarks have electric charges, they also interact via the electromagnetic force and the weak nuclear force.

Leptons

The six leptons are electron, electron neutrino, muon, muon neutrino, tau and tau neutrino. The electron, muon and tau leptons have electric charges and are influenced by electromagnetism. They all carry a $-1e$ electric charge, while their respective antiparticle have electric charge $+1e$. Every lepton also carry a lepton number, which is conserved in all known interactions, and a weak isospin such that they interact weakly. Both leptons and antileptons have their respective lepton number +1 and -1, and each flavor has each own lepton flavor number with the same values as the lepton numbers. There are three generations where the three electromagnetic leptons are paired with their respective neutrino, and the masses of these three leptons increases with the generation. Only the electron (1st gen) is stable and doesn't decay, while the muon and tau leptons decay via the weak interaction. The first generation can contribute to the production of stable hadrons.

1.2 Neutrinos

The three neutrinos (electron, muon, tau) are a little more special than the other elementary particles. They are classified as leptons with half-integer spins, but they do not carry any charge and are then neutral. So they only interact via the weak nuclear force, making them very hard to track since they go through almost everything even though they are stable particles. There are some theories on if the neutrinos have antiparticles (Dirac) or if they are Majorana neutrinos. If they are Majorana, then they are the only fermions that are Majorana since all the other fermions have some electric charge. By detection of neutrinos and antineutrinos, it is only found neutrinos with left-handed chirality while antineutrinos are found with right-handed chirality. This comes from the weak interaction where the parity is broken. From the weak nuclear force mediator particles, the $W^{\pm}$ bosons, we know that they only couple to left-handed particles and right-handed antiparticles. This means that interaction of the right-handed neutrinos is not covered in the Standard Model. Since mass terms couple both left- and right-handed states, the neutrinos are considered as massless in the Standard Model. It is therefore not clear if neutrinos have a mass or not yet, but it is thought from experiments that they have a very small mass at least. Through the discovery of neutrino oscillations [8], we know that the neutrinos can change flavor given proper conditions to a different type of neutrino, meaning they cannot be massless. So, one type of neutrino can in fact change flavor to another type of neutrino when it travels over a large distance. This neutrino oscillation describes the difference of the neutrino flavor eigenstates and the neutrino mass eigenstates. This type of physics is not covered by the Standard Model and will be looked more into later.

1.2.1 Neutrino Oscillations

From the Standard Model we know that for all interactions the lepton number is conserved for both the total and each lepton flavor separately in beta-decay. So the lepton number is then conserved when a $W^{\pm}$ boson decays into a lepton/associated lepton neutrino pair.

The discovery of the neutrino oscillations have been done by several experiments. The two biggest contributions to the discovery of the neutrino oscillations came from the Super-Kamiokande Observatory and the Sudbury Neutrino Observatories (SNO) experiments. They got the Nobel Prize in physics in 2015 for their contributions by detecting solar neutrinos from β-decay in the Sun [9]. The Super-Kamiokande detected electron neutrinos using a big water Čerenkov detector, but they got a too low electron neutrino flux than what was expected to be produced in the Sun. The SNO experiment showed that the atmospheric neutrinos and the neutrino flux from β-decay in the Sun had strong muon and tau components by using heavy water. This meant that the solar neutrinos could be measured with different physical processes for the neutrino flavors. Since only electron neutrinos are produced by nuclear fusion in the Sun, the neutrinos have to have the ability to change their flavor when moving over large distances.

The neutrino oscillation is a quantum-mechanical phenomenon, where the neutrino flavor (weak) eigenstates $(\nu_e, \nu_\mu, \nu_\tau)$ can be related to the mass eigenstates (ν_1, ν_2, ν_3) by an unitary transformation matrix U as

$$\begin{pmatrix} \nu_e \\ \nu_\mu \\ \nu_\tau \end{pmatrix} = \begin{pmatrix} U_{e1} & U_{e2} & U_{e3} \\ U_{\mu 1} & U_{\mu 2} & U_{\mu 3} \\ U_{\tau 1} & U_{\tau 2} & U_{\tau 3} \end{pmatrix} \begin{pmatrix} \nu_1 \\ \nu_2 \\ \nu_3 \end{pmatrix}.$$

So the flavor eigenstates are linear combinations of the mass eigenstates. The 3×3 unitary matrix is the Pontecorvo-Maki-Nakagawa-Sakata (PMNS) matrix, and it's expressed with three mixing (rotation) angles and a complex Dirac CP violation phase. The unitary of the PMNS matrix implies that $U^{-1} = U^\dagger \equiv (U^*)^T$ and $UU^\dagger = I$.

If the neutrino mass eigenstates are not the same, we get neutrino oscillations from the phase differences in components of the wavefunction. Since we already know that the neutrinos change flavor from the discovery of neutrino oscillations, we know that the neutrinos need some mass, differing by flavor, to being able to change flavor. That is why at least two of the neutrinos need non-zero masses and not the same for neutrino oscillations to be true. From experimental measurements, like long baseline accelerators, for the neutrino masses there is only found upper limits to the masses. The upper limits on the neutrino masses is found to be

$$\sum_{i=1}^{3} m_{\nu_i} \lesssim 1\text{eV}. \tag{1.1}$$

The reason why the neutrino masses seems to be so much smaller than the other fundamental particles is not known or covered by the Standard Model to this date.

1.3 Symmetries

Particle dynamics are heavily influenced by symmetries and laws of conservation. From classical Newtonian physics, we know that energy (E), three-momentum ($\vec{p}$) and total angular momentum (J) are conserved quantities. This is also the cause in the Standard Model. A quantity that is not conserved is the (rest) mass (m). This is something we know according to Einstein's Special Relativity. This leads to the ability to produce heavier particles in particles colliders than the particles used to collide at the start.

Another fundamental symmetry of physical laws is the CPT theorem. The CPT theorem is one of the results concluded by Quantum Field Theory, and states that all physical processes are symmetric under CPT-transformation [10]. C is charge conjugation, where every particle can be replaced by its antiparticle. P is parity reflection, where everything in the universe is mirrored along the three physical axes. T is time reversal, where the direction of time is reversed in the sense of looking at the local properties of the Standard Model. The combination of these three symmetries is predicted by the Standard Model to be a symmetry, while each symmetry alone is only a near-symmetry. The CPT symmetry gives rise to that particles and antiparticles have identical masses, magnetic moments, etc. The CPT is also thought to ba an exact symmetry in the Universe. Only the weak interactions of quarks and leptons seems to violate the C-, P-, T- and CP-symmetries out of the three fundamental forces explained by the Standard Model.

A topic to be further discussed later is gauge theory (sect. 1.4.2). From the connected gauge symmetry in the Standard Model, we get a conservation of certain quantum numbers during the different interactions with the fundamental forces based on the $SU(3) \times SU(2) \times U(1)$ group. The conserved quantities that are conserved are: the color charge for the strong nuclear interaction ($SU(3)$), the electric charge for electromagnetic interactions ($U(1)$) and the weak isospin for the weak nuclear interaction ($SU(2)$).

Other important conservation laws are the conservation of baryon number, B, and lepton number, L_x, in an interaction. x is the lepton flavor. The only case where the lepton number is not conserved is for neutrino oscillation. As we have explained earlier, neutrinos can change flavor when traveling large distances. But, this is not something we have to be concerned about in our case.

1.4 Quantum Field Theory

To explain the Standard Model as we know it today, we need quantum field theory (QFT). This is a theory that combines quantum mechanics, special relativity and field theory. In other words, quantum field theory tries to explain the little things in the universe, like the elementary particles, that move very fast, close to or with light speed c. This also says that every elementary particle has its own associated field. These fields can then be explained in terms of the Lagrangian density, $\mathcal{L}$, to explaining the dynamics and kinematics of the fields.

The combination of quantum mechanics and special relativity does give some problems. The most important equation in quantum mechanics is the Schrödinger equation, and it's not Lorentz invariant. The problem with this is that Schrödinger's equation is not the same for two observers in different reference frames. Other problems this leads to is that we get violation of causality, negative energy states and there is no possibility for new particle creations. The good thing is that these problems can be fixed by exchanging the Schrödinger equation (see Notation and Conventions) by the Dirac equation [11][12] for $\frac{1}{2}$-spin particles and the Klein-Gordon equation [11][12] for scalar particles. With the Dirac and Klein-Gordon fields, this leads to specific (gauge) theories for different particles and associated interactions, which we have briefly mentioned earlier and will explain more soon.

1.4.1 The Lagrangian

For more simple classical mechanics cases the Lagrangian is just given as the difference between the kinetic energy and the potential energy, $L = K - V$. This is also a baseline for the quantum field theory. By using the Lagrangian of a system with a set of generalized coordinates q_i and their time derivatives $\dot{q}_i$, we can find the equation of motion that describes the system by using the Euler-Lagrange equation,

$$\frac{d}{dt}\left(\frac{\partial L}{\partial \dot{q}_i}\right) - \frac{\partial L}{\partial q_i} = 0. \tag{1.2}$$

A difference for quantum field theory is that instead of kinetic and potential energies, or the generalized coordinates, we use fields with four space-time coordinates. This changes the Lagrangian L to the Lagrangian density $\mathcal{L}$ as a continuous system. This is a function of the fields, $\phi_i(t,x,y,z)$, and their derivatives, $\partial_\mu \phi_i(t,x,y,z)$. Since L is the spatial integral over $\mathcal{L}$,

$$L = \int \mathcal{L} d^3\mathbf{x}, \tag{1.3}$$

and using the principle of least action [13], the new Euler-Lagrange equation becomes

$$\partial_\mu \left(\frac{\partial \mathcal{L}}{\partial(\partial_\mu \phi_i)}\right) - \frac{\partial \mathcal{L}}{\partial \phi_i} = 0. \tag{1.4}$$

For simplicity we will just call the Lagrangian density as the Lagrangian from now on. From this new Euler-Lagrange equation, we can derive both the free-particle Dirac and the Klein-Gordon equations by imposing the Lagrangian with a free fermion field[1] and free theory[2] respectively. The Lagrangian for the spin-half (spinor) field, ψ, is

$$\mathcal{L}_D = i\bar{\psi}\gamma^\mu \partial_\mu \psi - m\bar{\psi}\psi, \tag{1.5}$$

and the Lagrangian for the non-interacting scalar field, ϕ, is

$$\mathcal{L}_S = \frac{1}{2}(\partial_\mu \phi)(\partial^\mu \phi) - \frac{1}{2}m^2\phi^2. \tag{1.6}$$

[1] Relativistic spin-half fields, Chapter 17.2.2 in Thomson [1]
[2] Relativistic scalar fields, Chapter 17.2.2 in Thomson [1]

Both of these two equations for the Lagrangian contain a kinematic term and a mass term.

With perturbation theory in quantum mechanics, the Lagrangian can also be used to describe the behavior and interaction of elementary particles with Feynman diagrams for simpler visualization of usually complex particle interactions.

1.4.2 Qauge Theories

To further explain the interactions between the elementary particles, which we now know from the new Lagrangian varies depending on the particles and associated interactions, we need a new theory. In this theory we need to require that the Lagrangian stays invariant under local transformations using symmetry or gauge groups. In special relativity, this global symmetry group is called the Poincaré group which includes spacetime symmetries.

To describe the Standard Model we need an internal gauge invariant symmetry that represents the different elementary interactions and is independent of spacetime coordinates, and this is the local $SU(3) \times SU(2) \times U(1)$ gauge symmetry group (Lie group). Here each special unitary group with degree n (the number in the parenthesis) is connected to its own gauge theory and the three elementary interactions in the Standard Model, and n is a n-dimensional space. If a symmetry group is commutative, meaning that regardless of what the order of the elements are applied the result will be the same, then it is called an Abelian group. If the group is non-commutative, it is then a non-Abelian gauge theory which implies the existence of gauge boson self-interaction.

Quantum chromodynamics (QCD)

The gauge theory that defines the strong interaction between the quarks and (eight) gluons (color charged particles) is the quantum chromodynamics sector [14]. The QCD conserves the separately conserved color charges red, green and blue, and thus works in a three dimensional color space. Another quantity that is conserved in QCD is parity. This comes from that the QCD interaction Hamiltonian is invariant under parity transformations (sect. 11.2.2 in Thomson [1]). The antiquarks carry the opposite color charge to the quarks of red, green and blue. The color states consists of color isospin and color hypercharge. It also ensures invariance under the local gauge transformation. The gauge symmetry group for this sector is $SU(3)_C$ and is represented by 3×3 matrices, where the C stands for the conserved color. This symmetry group does not commute and is then non-Abelian gauge theory, or more precise it is a Yang-Mills gauge theory [15]. By using this gauge theory, we can derive a new invariant Lagrangian which does not have a mass term for the gluons:

$$\mathcal{L}_{QCD} = \bar{\psi}(i\gamma^{\mu}\partial_{\mu} - m)\psi - \frac{1}{2}g_s\bar{\psi}\gamma^{\mu}\lambda_a\psi G^a_{\mu} - \frac{1}{4}G^a_{\mu\nu}G^{\mu\nu}_a \tag{1.7}$$

ψ is a fermion (quark) field, g_s is a coupling constant of the strong interaction, γ^{μ} are Dirac matrices, $a = 1, ..., 8$ is the eight gluons, λ_a is one of the eight Gell-Mann matrices and $G^a_{\mu\nu}$ is a gauge invariant gluon field strength tensor. This Lagrangian (eq.1.7) implies that the gluons should be massless and can self-interact.

In Figure 1.3 we see the QCD vertices for quark and gluon interactions (and self-interacting gluons) as seen by writing out the new Lagrangian (eq. 38 in Ecker [14]).

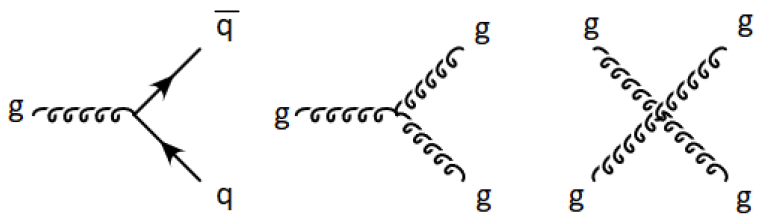

Figure 1.3: Here we see Feynman diagrams of the basic QCD vertices. From left to right we see, the coupling of gluon fields (g) interaction with quark fields (q), a triple gluon vertex and a quartic gluon vertex. Source Fig. 10.1 in Thomson [1].

Quantum electrodynamics (QED)

The gauge theory that defines the electromagnetic interaction for the electrically charged particles and photons is the quantum electrodynamics sector [16]. The QED conserves the electric charge of the particles, and the antiparticles have opposite electric charge to the particle. Like in QCD, parity is conserved in QED (sect. 11.2.2 in Thomson [1]). The gauge symmetry group for this sector is $U(1)$ and is an Abelian group. By starting with a free fermion field for the Lagrangian (eq.1.5, is invariant under *global* $U(1)$transformation) and make it invariant under the local phase transformation. This leads to a Lagrangian with a Lorentz-invariant description where there is an electromagnetic interaction between fermions and the gauge field of the massless photon:

$$\mathcal{L}_{QED} = \bar{\psi}(i\gamma^\mu \partial_\mu - m_e)\psi + e\bar{\psi}\gamma^\mu\psi A_\mu - \frac{1}{4}F_{\mu\nu}F^{\mu\nu} \tag{1.8}$$

ψ is the field of the half-spin particles, e is a coupling constant of the electromagnetic interaction, γ^μ are Dirac matrices, A_μ is a covariant four-potential (gauge field), and $F_{\mu\nu}$ is an electromagnetic field strength tensor.

From this Lagrangian (eq.1.8) we can get the Feynman diagram of the QED interaction vertex in Figure 1.4 between a single photon and two spin-half fermions.

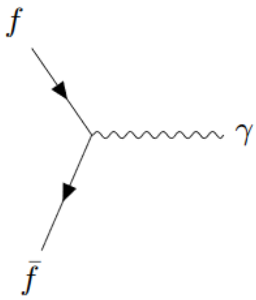

Figure 1.4: Here we see a Feynman diagram of the basic QED vertex of the interaction between fermions (f) and a massless photon (γ). Source Fig. 5.6 (and 10.10a) in Thomson [1].

Electroweak theory (EWT)

The gauge theory that defines the weak interaction for the flavor charged particles and the W and Z bosons/fields is the quantum flavordynamics (QFD) sector. Unlike QCD and QED, it is found experimentally that parity is not conserved in the weak interaction (sect. 11.2.3 in Thomson [1]). This parity-violation makes the weak interaction treat left-handed and right-handed particles differently. The charge-current weak interaction is invariant under $SU(2)$ local phase transformations and includes weak isospin.

The cross-section of W-pairs produced at higher energies, violates quantum mechanical unitarity such that particle probability is no longer conserved. At these higher energies, the electromagnetic and weak interactions become more and more similar in strength. That is why a unification of these two interactions is more used in particle physics, and it introduces the neutral Z boson as the solution to the cross-section. This unified theory is known as electroweak theory [17] or Glashow-Weinberg-Salam (GWS) theory. This theory (from the 1960's) earned the three contributors Glashow[18], Weinberg[19] and Salam[20] the Nobel Prize in Physics in 1979 [21][22]. What makes the EWT theory more complicated than the QCD and QED theories is that the fermions exists as left- and right-handed chirality states, while W-bosons only couple to left-handed fermions. The EWT conserves the flavor charge and weak isospin of the particles. It is this introduced weak isospin quantum number that accounts for the W-boson coupling, since left-handed fermions have half-isospin and appears as isospin doublets while right-handed fermions appear as isospin singlets. Something to take notice of here is that, the weakly interacting quarks are superpositions of the mass eigenstates while the strongly interacting quarks are mass eigenstates.

The electroweak theory is based on the $SU(2)_L \times U(1)_Y$ symmetry group, where L is left-handed interaction and Y is the weak hypercharge consisting of an electric charge Q and the third component of the weak isospin I_3, $Y = 2(Q - I_3)$. This new $U(1)_Y$ local gauge symmetry is used instead of that in QED, where the charge now has been replaced by the weak hypercharge. Each gauge invariant transformation in this theory, introduce new gauge fields which as linear combinations corresponds to the photon and W and Z bosons of the weak interaction. With these new gauge fields, we can derive yet another new preliminary (electroweak) Lagrangian that is associated with the EWT theory:

$$\begin{aligned}\mathcal{L}_{EWT} =& \bar{\psi}_L \gamma^\mu \left[i\partial_\mu - \frac{1}{2} g \boldsymbol{\sigma} \mathbf{W}_\mu - \frac{1}{2} g' Y B_\mu \right] \psi_L + \bar{\psi}_R \gamma^\mu \left[i\partial_\mu - \frac{1}{2} g' Y B_\mu \right] \psi_R \\ & - \frac{1}{4} B_{\mu\nu} B^{\mu\nu} - \frac{1}{4} \mathbf{W}_{\mu\nu} \mathbf{W}^{\mu\nu} \end{aligned} \tag{1.9}$$

$\psi_{L,R}$ are the fields for left- and right-handed fields respectively, g and g' are coupling constants related to the elementary charge, γ^μ are the Dirac matrices, $\boldsymbol{\sigma}$ are the Pauli matrices, B_μ is a field strength tensor for the weak hypercharge gauge field for $U(1)_Y$, $\mathbf{W}_{\mu\nu}$ is a field strength tensor for the three weak isospin gauge fields for $SU(2)_L$. We also have to account for the left- and right-handed states such that we don't destroy the gauge invariance, like including the fermion mass term that mixes the left- and right-handed fields. The complete EWT Lagrangian will be looked at soon.

This EWT gauge symmetry group is non-Abelian, and a Yang-Mills gauge theory. In Figure 1.5 and 1.6 we see Feynman diagrams of the electroweak interaction vertices including fermions and gauge boson self-interactions we get from the Lagrangian in equation 1.9. There we see that the photon and the Z-boson couple with both left- and right-handed fermions, while the W-bosons do not. Here we have described the interactions between the fields even though the Lagrangian (eq.1.9) does not contain any mass terms, making it not fully complete since we know that fermions have mass and that W and Z bosons are massive.

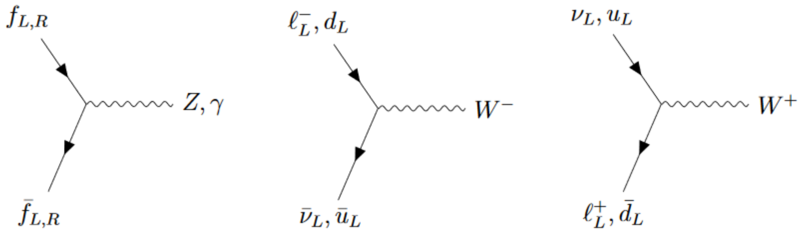

Figure 1.5: Here we see Feynman diagrams of the electroweak interaction vertices that includes fermions.

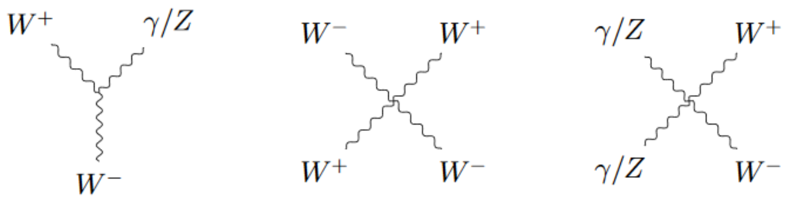

Figure 1.6: Here we see Feynman diagrams of the electroweak interaction vertices for gauge boson self-interaction.

1.4.3 Higgs Mechanism

As mentioned in the Higgs boson section 1.1.2, it is the Higgs boson that contributes to the masses of the fundamental particles in the Standard Model that have mass, by creating the quantum scalar Higgs field in the vacuum in all of space. Leptons and bosons interact differently with the Higgs field, where the W and Z bosons acquire masses when the Higgs field has a vacuum expectation value at a critical temperature. Up till this point, the Lagrangians do not contain any mass terms yet since these terms would break up the symmetry and gauge invariance needed. With the Higgs mechanism, which is also called the Brout-Englert-Higgs mechanism, the Higgs field is used to explain the masses of the bosons in the electroweak theory without breaking the local gauge symmetry. This concept is based on what is called spontaneous symmetry breaking.

Spontaneous symmetry breaking

In the lowest energy state of a field we find the minimum of a potential. This is also called the vacuum state. The requirements for the three gauge theories discussed is that the Lagrangian is invariant under local transformations of these theories, and that does not happen when we include the mass terms. The fermions will consistently develop mass, while the weak interaction bosons will emerge when at lower energies.

For a **real scalar field**, there are two cases we have to consider. One is where we have $\mu^2 > 0$, where μ is the mass, which gives the vacuum expectation value to zero. Remember that the Lagrangian is kinetic terms minus potential terms, and that the vacuum expectation value is defined as the minimum of the potential. In this case we have a finite minimum. Under these circumstances, we have invariance under transformation and symmetry of the Lagrangian. In the other case when $\mu^2 < 0$, the vacuum expectation value is non-zero and the previous mass term need a new interpretation. Here we have several minima, one with $+$ sign and one with $-$ sign. Since we have a choice of vacuum state, this breaks the symmetry of the Lagrangian. This is spontaneous symmetry breaking. The potential and the Lagrangian are still symmetric under transformation, but because of the new interpretation of the mass term we need to rewrite the Lagrangian to a state with zero as vacuum expectation value. A new field is introduced which makes the Lagrangian no longer symmetric under field transformation, but now contains a mass term again. The Lagrangian is now expressed as the excitation of one of the minima where the field is interpreted as small perturbations about the chosen vacuum state.

For a **complex scalar field**, we consider the two same cases as above. With a complex scalar field, the Lagrangian is symmetric under global $U(1)$ transformations. For the first case ($\mu^2 > 0$) with the complex scalar field split into to real scalar fields, the symmetry of the Lagrangian is also conserved here when the two scalar fields are zero. This has an expected vacuum value of zero. For the second case ($\mu^2 < 0$), the potential gets an infinite amount of minima which forms a circle in the 2D-field plane known as the "Mexican hat"-potential. This vacuum state breaks the global $U(1)$ symmetry. With a reasonable set of variables for the vacuum state, we introduce two new fields which is used to describe the first complex scalar field. The Lagrangian now contains terms where one can be interpreted as a mass term and some as interaction terms. This Lagrangian ends up with a massive scalar field and a massless scalar field. The massless field is called a Goldstone boson, which comes from the Goldstone theorem [23] that states that a massless field will appear whenever a continuous symmetry is spontaneously broken.

The Brout-Englert-Higgs mechanism

To get to a theory with massive gauge bosons, we need to look at spontaneous symmetry breaking for local electroweak gauge theory. This theory that gives the gauge bosons mass without breaking the gauge theory is known as the Brout-Englert-Higgs mechanism. First we look at local $U(1)$ symmetry breaking, and then we look at the complete local $SU(2)_L \times U(1)_Y$ gauge group.

Local $U(1)$ symmetry breaking: We look first at a complex scalar field ϕ with a potential and require that the Lagrangian is invariant under the local gauge transformation. This basically leads to the QED Lagrangian for a scalar field (eq.1.8), but with an extra self-coupling term. When we compare with the second case, $\mu^2 < 0$, in the spontaneous symmetry breaking, tha vacuum state is degenerate and the $U(1)$ symmetry is spontaneously broken by the vacuum state. We now introduce two new fields η and ξ used to rewrite the Lagrangian. The breaking of the symmetry has now lead to a massive scalar field η and a massless Goldstone boson ξ. The previously massless gauge field A_μ has now acquired a mass term, giving the gauge bosons of the local gauge symmetry mass.

This rewritten Lagrangian has a few problems we need to look more into. First, an extra degree of freedom seems to have been introduced by the added mass term. Second, there is a term coupling the Goldstone field ξ and the gauge field A, meaning that the spin-1 gauge field can change into a spin-0 scalar field. The solution to these problems is to use a Unitary gauge, which changes the transformations under $U(1)$. The complex scalar field is now chosen to be a real field. The Lagrangian now contains two massive fields, the (scalar) Higgs field h and the gauge field A. It also contains Higgs self-interaction terms and interaction terms between the Higgs boson and gauge boson. The Goldstone boson has now disappeared from the Lagrangian.

Local $SU(2)_L \times U(1)_Y$ symmetry breaking: For the $SU(2)_L \times (U1)_Y$ local gauge symmetry, the simplest Higgs field consists of two complex scalar fields which are placed in a weak isospin doublet. The Lagrangian with this complex scalar double contains a Higgs potential. Once again to break the symmetry in the ground state, a choice of $\mu^2 < 0$ must be taken. The Higgs doublet will now be expressed in the unitary gauge, giving a Salam-Weinberg model Lagrangian. By writing the Lagrangian to respect the $SU(2)_L \times U(1)_Y$ local gauge symmetry of the electroweak model, the mass terms can be achieved. The Lagrangian now contains three massive gauge fields for $W^{\pm}, Z^0$, one massless gauge field B_μ and a massive scalar field h. The massless neutral gauge boson can be identified as the photon, while the other masses are

$$m_H = \sqrt{2\lambda}v, \quad m_W = \frac{1}{2}g_W v, \quad m_Z = \frac{1}{2}v\sqrt{g_W^2 + g'^2}, \tag{1.10}$$

which depends on the vacuum expectation value of the Higgs field v (found to be 246 GeV), the coupling constant of the $SU(2)_L$ gauge interaction g_W, the coupling constant of the $U(1)_Y$ gauge interaction g'^2 and the free Higgs potential parameter $\lambda > 0$.

The EWT theory, in addition to the coupling in Figure 1.5 and 1.6, now contains coupling between the Higgs boson and the massive gauge boson and Higgs self-interaction. These couplings can be seen in Figure 1.7.

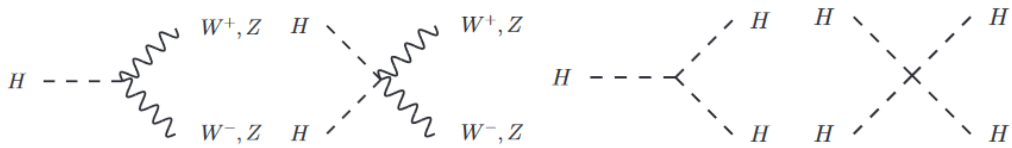

Figure 1.7: Here we see Feynman diagrams of the couplings between the Higgs boson and the massive gauge bosons and Higgs self-interaction.

Fermion masses: The Higgs mechanism can also be used to give masses to the fermions as well as the gauge bosons. The Higgs isospin doublet has a lower and an upper element. The lower element is used to give masses to down-type quarks and charged leptons, while the masses of the up-type quarks are constructed from the conjugate doublet. The gauge invariant mass terms of the Dirac fermions are then described as

$$m_f = \frac{g_f v}{\sqrt{2}}, \tag{1.11}$$

where g_f is the Yukawa coupling constant of the fermions to the Higgs field.

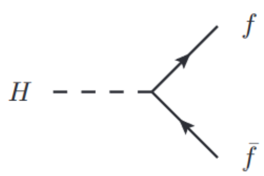

Figure 1.8: Here we see Feynman diagrams of the coupling between the Higgs boson and fermions.

Full EWT Lagrangian

With all the theory for the EWT theory we have covered, we can develop the full EWT Lagrangian:

$$
\begin{aligned}
\mathcal{L}_{EWT} =& \overline{\psi}_L \gamma^\mu \left[i\partial_\mu - \frac{1}{2} g \boldsymbol{\sigma} \mathbf{W}_\mu - \frac{1}{2} g' Y B_\mu \right] \psi_L + \overline{\psi}_R \gamma^\mu \left[i\partial_\mu - \frac{1}{2} g' Y B_\mu \right] \psi_R \\
& - \frac{1}{4} B_{\mu\nu} B^{\mu\nu} - \frac{1}{4} \mathbf{W}_{\mu\nu} \mathbf{W}^{\mu\nu} + \left| \left(i\partial_\mu - \frac{1}{2} g \boldsymbol{\sigma} \mathbf{W}_\mu - \frac{1}{2} g' Y B_\mu \right) \phi \right|^2 \\
& - V(\phi) - (g_f \overline{\psi}_L \phi \psi_R + G'_f \overline{\psi}_L \phi_c \psi_R + h.c.)
\end{aligned} \tag{1.12}
$$

The first line is the couplings between the fermions and the gauge fields and kinetic terms for the fermion fields. The second line is the kinetic terms for the gauge fields and the Higgs field, the couplings between the gauge field and the Higgs field, and the couplings between the gauge fields. The third line contains the scalar potential, the Yukawa coupling terms and the fermion mass terms, and $h.c$ stands for the corresponding Hermitian conjugate.

Chapter 2

Theories Beyond the Standard Model

The Standard Model is just a theory that seems to explain a lot of the physics in the Universe we see from experiments, like the theory we have covered earlier with the interaction between the elementary particles and how some have mass. The Standard Model can be seen as a model with many (25 or so) free parameters that are chosen to match our observations. But it does not explain everything, like the existence of the graviton and gravity and more. To goal for most researchers is now to try and extend the SM to a Unified field theory or a Theory of everything, that explains all the physical phenomena which the original SM does not.

One of these things is that we only seem to know what about 5% of the matter in the Universe are. This 5% of the matter in the Universe is visible to us, called baryonic matter, while the rest is something yet unknown. One theory is that the about 25% is something called dark matter, that acts as matter and has a gravitational pull in the Universe. It is thought that if dark matter is a particle and since it has a gravitational effect on baryonic matter, it must have a mass. This is seen by looking at galaxies in the Universe where the visible mass alone can't contribute to the observed velocity distributions of stars in galaxies. Since we can't seem to detect any electromagnetic radiation of dark matter, it is thought that they do not have any electric charge. So the neutrino seems like a candidate that could fit. But studies and computer simulations show that this would lead to a *hot dark matter* universe, whereas observations show that the universe must have *cold dark matter* to explain the galaxy formations. Other cosmological observations also provide evidence of this dark matter, but no concrete results of what this actually is have been presented to this date. The remaining 70% is then thought to be dark energy, which has a pushing affect on the galaxies in the Universe making it expand faster and faster with time as it seems now. This we know even less about what could be.

When one looks closer at the Standard Model, one can suspect that there might be some underlaying symmetry principle unifying some of the free SM parameters mentioned. The Supersymmetry theory goes beyond the SM and predicts the existence of weakly interacting massive particles (WIMPs) as an extension to the SM, which might be (cold) dark matter particles with masses in the range of a few GeV to TeV. Supersymmetry is one of the hot and bigger theories in particle physics today, where much of the focus is to observe these WIMP particles through production at the LHC (more in section 4) or as direct detection in galaxies.

We will look more into this and a few other aspects and theories about the neutrino in this chapter which the classic SM does not cover.

2.1 Supersymmetry

One of the more popular extensions to the SM is Supersymmetry(SUSY) theory, and the Minimal Supersymmetric Standard Model (MSSM) [24] with a minimal amount of new particles introduced. The foundation for this theory is that each particle in the SM has a super-symmetric partner, *sparticles*, with half a unit spin difference. The fermion superpartners are called *sfermions* and are spin-0 scalars, and similarly for the spin-1 gauge fields their superpartners are called *gauginos* with spin-half. Fermions get an "*s-*" in front of their name, while gauge fields gets an "*-ino*" ending. They are denoted with a tilde sign above their names, such that the superpartner for a W-boson is a *wino* $\widetilde{W}$. These sparticles are yet to be discovered. The mass and other properties of the SM particles would have been the same for their respective superpartner if SUSY was an exact symmetry. Since these superpartners have not been discovered yet, the masses can't be the same. Meaning that SUSY must be a broken symmetry and that the sparticles must be heavier than the SM particles since they have not been discovered in experiments yet. The mass scale is theorized to $\mathcal{O}(1\text{ TeV})$.

One property of SUSY is that the bosons and fermions are related by a SUSY operator that commutes with the SM gauge transformations, and no new forces introduced. These representations of the gauge groups with their superpartners form supermultiplets. This leads to distinct superpartners for left- and right-handed fermions since they belong to different supermultiplets. SUSY particles will always be produced in paris in particle colliders to conserve a quantity called $R-parity$ [25], which we will not explore more here. One of the dark matter candidates are the lightest supersymmetric particles

(LSP) and they must be stable, and in MSSM this is the lightest neutralino as a WIMP. The LSP is a result of several decays from sparticles. SUSY particles have not been detected in particle colliders yet, since the LSPs are neutral they avoid detection. But they can be detected as missing transverse energy, since the total transverse energy must be conserved after collision.

SUSY is not a complete and simple theory for the full theory of the nature. Although, it seems that many quantum theories involving gravity might need SUSY as an ingredient to make sense. The big and exciting problem now is to detect these sparticles in experiments, thus proving the theory.

2.2 Neutrino Masses

According to the Standard Model, neutrinos do not have mass. This happens because the SM only covers left-handed neutrinos, since the right-handed neutrinos do not involve in any of the fundamental interactions in the model and have not been observed so far. As mentioned earlier, we know from observations and experiments of neutrino oscillations that neutrinos have to have some mass to being able to change flavor when moving over large distances. This neutrino masses is something we need to look more into.

2.2.1 Dirac Neutrinos

Dirac particles are particles which can be distinctively separated from its antiparticle. The Dirac field is described by a four-component Dirac spinor ψ and can be divided into a left-handed ψ_L and a right-handed ψ_R part as two component Weyl spinors:

$$\psi = \begin{pmatrix} \psi_L \\ \psi_R \end{pmatrix}. \tag{2.1}$$

The left-handed neutrinos in the Standard Model are then described by this left-handed Weyl field. Since the Dirac mass term require both left- and right-handed fields in the SM, there is no Dirac mass term for the neutrinos.

If we assume neutrinos as Dirac particles, the neutrino mass is added similarly to the up-type quarks as the conjugate Higgs doublet. The gauge invariant Dirac neutrino mass term after spontaneous symmetry breaking becomes

$$\mathcal{L}_D = -m_\nu(\overline{\nu_R}\nu_L + \overline{\nu_L}\nu_R), \tag{2.2}$$

with the neutrino mass still determined by the Yukawa coupling constant as for Dirac fermions (eq. 1.11):

$$m_\nu = \frac{g_\nu v}{\sqrt{2}} \tag{2.3}$$

The neutrino masses have been found to be several orders of magnitude smaller than the charged lepton masses. This leads to a Yukawa coupling constant $g_\nu \leq 10^{-12}$ for neutrino masses that are less than 1 eV (sect. 1.2.1). It is not known why this Yukawa constant is so small, which gives reason to that there must be something else that gives the neutrinos their masses. From this the right-handed neutrino in the SM would be sterile and only interact with the Higgs boson.

2.2.2 Majorana Neutrinos

Another option for the neutrinos, is that they can be Majorana neutrinos. This means that they can be their own antiparticles. The result of this would mean that the lepton number no longer is conserved, which it is in the SM. To not break the gauge invariance of the SM when adding the fields for RH neutrinos and LH antineutrinos in the Lagrangian, the LH antineutrinos appear as the CP conjugate field of the RH neutrino[1] defined by

$$\psi_L^c = \hat{C}\hat{P}\psi = C\overline{\psi}_R^T, \tag{2.4}$$

where C is the charge conjugation matrix.

For a Majorana neutrino we have $\psi^c = \psi$, which means that the neutrino field can be expressed with a Majorana spinor

$$\psi_\nu = \begin{pmatrix} \overline{\nu_R^c} \\ \nu_R \end{pmatrix} \tag{2.5}$$

for left-handed and right-handed neutrino fields and the CP conjugate of the right-handed field (or the left-handed antineutrino) $\overline{\nu_R^c}$. The local gauge invariant Majorana neutrino mass term, with Majorana mass M, becomes

$$\mathcal{L}_M = -\frac{1}{2}M(\overline{\nu_R^c}\nu_R + \overline{\nu_R}\nu_R^c). \tag{2.6}$$

This means that the Majorana mass term is not constrained by gauge symmetry and can be arbitrary large. The global baryon number minus the lepton number $(B - L)$ symmetry of the SM would be broken if the neutrino is a Majorana neutrino. From observations of the asymmetry between matter and antimatter in the Universe, it actually looks like the baryon number is not conserved.

2.2.3 The Seesaw Mechanism

One of many theories for the light masses of the neutrinos is to add right-handed neutrinos that couple to the left-handed neutrinos. However, this would lead to a disparity problem regarding mass scale remains. To solve this, a seesaw mechanism is introduced where the observed (light Dirac) left-handed neutrinos couple with very heavy (sterile) Majorana right-handed neutrinos. This would explain the small masses of the observed SM left-handed neutrinos and the absence of observation of right-handed neutrinos. The problem is that the mass scale of the right-handed neutrinos is unknown, since the masses of the Dirac neutrinos are still uncertain. So they could be somewhere between a few keV and possibly be light dark matter particles or have more heavy masses near the unification energy (GUT scale), where the electromagnetic, weak and strong forces have equal strength.

Type-I seesaw mechanism

There are several varieties of the seesaw mechanism which extends the SM, but the simplest one is the **Type-I seesaw mechanism**[26]. This involves the mix of left-handed Dirac neutrinos and right-handed Majorana neutrinos. In this theory there is added a right-handed neutrino for each of the SM left-handed neutrinos, in total three added right-handed neutrinos. When involving neutrinos as Majorana, we get that $\overline{\nu_L}\nu_R$ is equivalent to $\overline{\nu_R^c}\nu_L^c$. The Lagrangian after the spontaneous electroweak symmetry breaking with both the Dirac and Majorana mass terms becomes:

$$\mathcal{L}_{DM} = -\frac{1}{2}\left(m_D\overline{\nu_L}\nu_R + m_D\overline{\nu_R^c}\nu_L^c + M\overline{\nu_R^c}\nu_R\right) + h.c. \tag{2.7}$$

m_D is the Dirac mass and M is the Majorana mass. This equation can also be written in terms of a 2×2 mass matrix ($\mathcal{M}$) for the neutrinos:

$$\mathcal{L}_{DM} = -\frac{1}{2}(\overline{\nu_L}\overline{\nu_R^c})\begin{pmatrix} 0 & m_D \\ m_D & M \end{pmatrix}\begin{pmatrix} \nu_L^c \\ \nu_R \end{pmatrix} + h.c. \tag{2.8}$$

By looking at the eigenvalues (λ) of the mass matrix $\mathcal{M}$ we get the physical masses of the neutrinos (in this model) as (sect.17.8.1 in Thomson [1])

$$m_\pm = \lambda_\pm = \frac{M \pm M\sqrt{1 + 4m_D^2/M^2}}{2}. \tag{2.9}$$

If we assume the Majorana mass much larger than the Dirac mass, $M >> m_D$, we get a light left-handed neutrino state (ν) and a heavy right-handed neutrino state (N) with masses

$$|m_\nu| \approx \frac{m_D^2}{M} \quad \& \quad m_N \approx M. \tag{2.10}$$

The physical neutrino states are in this case

$$\nu \approx (\nu_L + \nu_R) - \frac{m_D}{M}(\nu_R + \nu_R^c) \quad \& \quad N \approx (\nu_R + \nu_R^c) + \frac{m_D}{M}(\nu_L + \nu_L^c). \tag{2.11}$$

By looking at equation 2.10, we see that the lightness of the SM neutrinos are explained when there exists much heavier right-handed neutrinos.

Inverse seesaw mechanism

The model we are studying involves a slightly different seesaw theory, namely the so-called **Inverse seesaw mechanism** [27][28]. This is a low-scale Type-I neutrino mass model and yields heavy neutrino masses and allow large Yukawa couplings. Besides the addition of right-handed neutrinos, this model also adds three singlet fermions. This then yields three light left-handed neutrinos and heavy pseudo-Dirac neutrinos[29][30] with small lepton number violations in the singlet mass terms. This comes from the decay of a $W_R^\pm$ to a pseudo-Dirac neutrino, since a neutrino coupled to a $W_R^\pm$ is a pseudo-Dirac fermion. It is during this process that the lepton number is approximately conserved, and accounts for missing same-sign electron events.

Our base model is the $SU(2)_L \times SU(2)_R \times U(1)_{B-L}$ left-right symmetry group (sect 2.3) which involves this inverse seesaw mechanism, and is based on the

$$SU(3)_C \times SU(2)_L \times SU(2)_R \times U(1)_{B-L} \tag{2.12}$$

gauge symmetry. The main difference from the Type-I seesaw mechanism is that instead of a heavy Majorana mass eigenstate neutrino, we have a heavy pseudo-Dirac neutrino mass eigenstate. The mass difference (mixing) between the left- and right-handed neutrinos probe small neutrino masses. This leads to Left-Right symmetric models with the same final state as for a heavy Majorana neutrino.

2.3 Left-Right Symmetry

The theory of the Left-Right Symmetric Model (LRSM)[31, 32, 33, 34, 35] was used first to explain the parity violation where there is low energy processes. By adding a right-handed part to the SM gauge symmetry, $SU(2)_R$, the LRSM tries to fix the parity symmetry at high energies. This is stated in Mohapatra [26]: "... *weak interactions like the strong and electromagnetic ones are parity conserving at very high energies and observed maximally parity violating V-A structure of low energy weak processes is a consequence of gauge symmetry breaking.*" This changes the electroweak gauge group to $SU(2)_L \times SU(2)_R \times U(1)_{B-L}$. In the SM, the electromagnetic charge goes as

$$Q_{em} = I_3{}^{3} + \frac{Y}{2}, \tag{2.13}$$

where Y is the weak hypercharge (as in sect.1.4.2). In the LRSM, the weak hypercharge factor in the electromagnetic charge is replaced with the difference between the baryon and lepton number, and a right-handed part of the weak isospin $I_3{}^{4}$ [26]. This changes the electromagnetic charge to

$$Q_{em} = I_{3L} + I_{3R} + \frac{B-L}{2}. \tag{2.14}$$

The left- and right-handed weak interactions of the fermion fields (**Q**uarks and **L**eptons) in the LRSM transforms as doublets

$$\mathbf{Q}_{L,R} = \begin{pmatrix} u_i \\ d_i \end{pmatrix}_{L,R} \quad \& \quad \mathbf{L}_L = \begin{pmatrix} \nu_i \\ e_i \end{pmatrix}_L, \quad \mathbf{L}_R = \begin{pmatrix} N_i \\ e_i \end{pmatrix}_R, \tag{2.15}$$

where $i = 1, 2, 3$ stands for the generation index in the SM (see Figure 1.1). We also get three gauge-singlet fermions, S_{L_i}, leading to chiral partner fields of N_{R_i}[28].

The Higgs sector in our symmetry model (eq. 2.12) has two Higgs multiplets. One is the Higgs $SU(2)_{L,R}$ multiplet $\Delta_L \times \Delta_R$. The other breaks the electroweak symmetry and is a $SU(2)_L \times SU(2)_R$ bi-doublet Φ with vacuum expectation value (VEV)

$$\langle \Phi \rangle = \begin{pmatrix} v_u & 0 \\ 0 & v_d \end{pmatrix}^{5}. \tag{2.16}$$

A $SU(3)_R$ doublet Higgs field H_R is also introduced to break down the $SU(2)_R$ symmetry, with VEV:

$$\langle H_R \rangle = \begin{pmatrix} 0 \\ v_R \end{pmatrix} \tag{2.17}$$

This breaks the left-right symmetry $SU(2)_L \times SU(2)_R \times U(1)_{B-L}$ down to the SM symmetry $SU(2)_L \times U(1)_Y$. We then get the fermion mass terms

[3] $I_3 = I_{3L}$. (weak isospin in the Standard Model)

[4] This means that the SM weak hypercharge factor really is $\frac{Y}{2} = I_{3R} + \frac{B-L}{2}$.

[5] $v = \sqrt{v_u^2 + v_d^2} \approxeq 174\text{GeV}$.

after this symmetry breaking. The VEV of H_R (eq.2.17) contributes both to the masses of heavy neutrinos and to the masses of the broken symmetry gauge bosons $W_R^{\pm}$ and Z_R[6] as:

$$m_{W_R} \approxeq \frac{g_R v_R}{\sqrt{2}} \quad \& \quad m_{Z_R} = \frac{\sqrt{g_R^2 + g_{B-L}^2}}{\sqrt{2}} v_R \tag{2.18}$$

This then leads to a weak interaction Lagrangian[28] for the $W - W_R$ mixing after the VEV of the bi-doublet Higgs field Φ has been acquired:

$$\mathcal{L}_{weak} = (W_L^- W_R^-) \begin{pmatrix} \frac{g_L^2 v^2}{2} & -\frac{g_L g_R v^2 \sin 2\beta}{2} \\ -\frac{g_L g_R v^2 \sin 2\beta}{2} & \frac{g_R^2}{2}(v_R^2 + v^2) \end{pmatrix} \begin{pmatrix} W_L^+ \\ W_R^+ \end{pmatrix} {}^{7} \tag{2.19}$$

This Lagrangian conserves parity prior to symmetry breaking.

[6]Both the gauge bosons are massive, but the $W_R^{\pm}$ gauge bosons have a charge while the Z boson is neutral.

[7]$\tan\beta \equiv \frac{v_d}{v_u}$.

Chapter 3

Proton-Proton Collisions

The base of what we are studying in this thesis, is the proton-proton (p-p) collision in chapter 5, like at the LHC (sect.4.2). Previously we have discussed that some of the elementary particles make up what we call hadrons, which protons are. This makes proton-proton collisions somewhat complex. When two hadrons collide, it is really a subset of the hadrons that collide. This subset is called partons, and can be quarks, antiquarks or gluons. Since it is effectively the partons that collide and not the protons, the partons only carry fractions of the total momentum of the protons. We also use the center-of-mass frame of the p-p collision system and not the center-of-mass frame of the patrons that collide. This chapter explains the basics of high energy proton-proton collisions.

3.1 Particle Kinematics

To describe the kinematics of what happens in p-p collisions, we need the momentum, energy and rest mass of the particles. The Einstein energy-momentum relation in natural units becomes

$$E^2 = p^2 + m^2. \tag{3.1}$$

Since the protons will reach very high velocities when they collide, we need to include special relativity into the equations[8]:

$$E = \gamma m \quad \text{and} \quad \mathbf{p} = \boldsymbol{\beta}\gamma m \tag{3.2}$$

These equations are dependent on the Lorentz factor

$$\gamma = \frac{1}{\sqrt{1-\beta^2}} \quad \text{and} \quad \beta = \frac{v}{c}.$$

[8]In natural units.

We then introduce the momentum as a four-vector momentum

$$P^\mu = (E, \mathbf{p}) = (E, p_x, p_y, p_z).$$

The scalar product of the four-momentum is then a Lorentz-invariant quantity

$$\begin{aligned} P^2 = P^\mu P_\mu &= E^2 - \mathbf{p}^2 \\ &= \gamma^2 m^2 - \beta^2 \gamma^2 m^2 \\ &= m^2, \end{aligned} \tag{3.3}$$

since the momentum and energy are conserved separately, the four-momentum is also conserved. Be rearranging this equation, we just end up with the Einstein energy-momentum relationship in equation 3.1. This is a very useful relation with particle collisions.

3.1.1 Colliding Particles

The reference frame of choice for colliding particles, is as mentioned the center-of-mass frame (CM) of the two colliding particles. This is defined where the sum of the three-momenta $\mathbf{p}$ is zero. When two particles collide, this means that $\mathbf{p}_1 = -\mathbf{p}_2$. And when these two particles have the same rest mass $E_1 = E_2 = E$, we get

$$(P_1 + P_2)^\mu = (2E, \mathbf{0}). \tag{3.4}$$

Now we introduce what is called a Mandelstam variable s [1], which is defined as the squared sum of the four-momenta

$$s = (P_1 + P_2)^2. \tag{3.5}$$

This we have already found out is a Lorentz-invariant quantity. We can then draw two conclusions; One, s is a Lorentz-invariant quantity as well, and two, the $\sqrt{s} = 2E$ can be interpreted as the total energy of the CM system. This is a key quantity in particle physics for particle colliders.

From equation 3.3, we got that $P^2 = m^2$. This means that we if the colliding particles were elementary particles, $\sqrt{s}$ could be interpreted as the possible energy available for heavier particle production. This would then be an upper limit for producing a heavy particle with mass M, as $M \leq \sqrt{s}$. But since protons are not elementary particles and the p-p collisions are really collisions between partons, this limit changes. We denote the momenta carried by the two partons colliding as $\mathbf{q}_1$ and $\mathbf{q}_2$. The associated four-momenta for the partons are Q_1^μ and Q_2^μ. Since we mentioned that the partons only carry fractions of the momenta, these fractions will be defined as x_1 and x_2 for the two colliding partons. By using what is called the Drell-Yan process (explained and derived in Thomson [1]) for a quark and an antiquark, we get the fractions given as

$$x_1 = \frac{q_1}{E} \quad \text{and} \quad x_2 = \frac{q_2}{E}. \tag{3.6}$$

To get the mass M of a produced particle from the collision with the partons, we use the same limit as for an elementary particle collision and equation 3.5 for s:

$$\begin{aligned} M &\leq \sqrt{s} \\ M^2 &\leq s \\ M^2 &\leq (Q_1 + Q_2)^2 = E^2 \left[(x_1 + x_2)^2 - (x_1 - x_2)^2 \right] \\ &= 4x_1 x_2 E^2 \\ &= x_1 x_2 s \end{aligned}$$

This leads to that the produced invariant mass is equal to the center-of-mass energy of the colliding partons.

The actual values of the fractions are given by their parton distribution functions (PDFs). These PDFs can be explained as the probability of a parton with a special flavor to carry the fraction x of the proton momentum when the parton participates in a hard scattering process. In hadron-hadron collisions, these scattered patrons can be observed as jets.

From this section, we can see that the event kinematics in hadron-hadron collisions have to be explained by the three independent kinematic variables, like Q^2, x_1 and x_2.

3.1.2 Products of Particle Collisions

In particle colliders, like at the LHC, the direction of the particle beams are normally defined in the z-direction which gives $\mathbf{p} = (0, 0, p)$. This plane is the longitudinal plane. The positive y-direction is defined upwards, and the positive x-direction is defined towards the center of the ring. We can then define the transverse momentum p_T perpendicular to the z-axis as

$$p_T = \sqrt{p_x^2 + p_y^2} = \sin\theta. \tag{3.7}$$

The corresponding transverse energy is given as

$$E_T = \sqrt{p_T^2 + m^2}. \tag{3.8}$$

The total momentum can then be derived as

$$p = \sqrt{p_T^2 + p_z^2}. \tag{3.9}$$

The reason for working in the transverse (xy) plane of the initial beam direction, is that the initial momentum is zero in this direction. We want to express the kinematics in spherical coordinates in terms of the polar angle θ and the azimuthal angle ϕ.

After the collisions, the parton jets will get a boost along the beam direction. That is why we introduce a *rapidity* variable y that is used to express the jet angles:

$$y = \frac{1}{2} \ln \left(\frac{E + p_z}{E - p_z} \right) \tag{3.10}$$

What is useful with this rapidity variable, is that the rapidity differences are invariant under Lorentz boosts along the beam direction. This does not apply for θ.

After what is called a hadronisation process, the invariant mass of the system of particles that forms a jet is referred to as the jet mass. If this jet mass is small compared to the jet energy, $p_z \approx E \cos\theta$. We can then rewrite the rapidity as

$$y \approx \frac{1}{2} \ln \left(\frac{1 + \cos\theta}{1 - \cos\theta} \right) = \frac{1}{2} \ln \left(\cot^2 \frac{\theta}{2} \right) = -\ln \left(\tan \frac{\theta}{2} \right) \equiv \eta \tag{3.11}$$

This new variable η is called the *pseudorapidity*. We now have the most used set of variables (p_t, ϕ, θ) for describing the kinematics of particles in a detector. In Figure 3.1 we see the illustration of the transverse and longitudinal planes. The cylindrical shape shows how particle accelerators will be situated around the collision point.

Another useful variable associated with hadron colliders, is the angular distance between two particles

$$\Delta R = \sqrt{(\Delta\eta)^2 + (\Delta\phi)^2}. \tag{3.12}$$

The angular distance defines how much two particles are moving in the same direction or as the separation in the $\phi\eta$-space, and is invariant under longitudinal boosts.

3.2 Proton-Proton Interactions

When proton-proton collisions take place in colliders, the interactions can be roughly be divided into three groups:

i) elastic (el) ii) diffractive (di) iii) non-diffractive (nd)

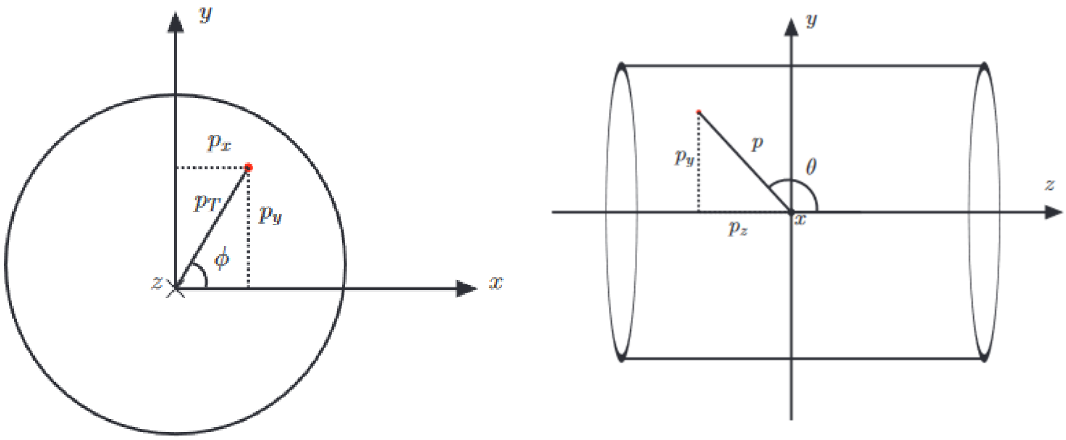

(a) The transverse plane. (b) The longitudinal plane.

Figure 3.1: Illustrations of the (a) transverse plane and the (b) longitudinal plane. The collision point is at the origin. Figures are both from ref. [36].

These three groups are also components that make up the total cross-section at proton-proton colliders:

$$\sigma_{\text{total}} = \sigma_{el} + \sigma_{di} + \sigma_{nd} \tag{3.13}$$

For elastic processes, both the colliding protons remain unchanged. For the diffractive processes (di and nd), the collisions/interactions are inelastic and one or both protons will be fragmented. This leads to multi-particle final states.

The elastic and diffractive interactions have cross-sections that can not be calculated using perturbation theory, meaning they are non-perturbative processes. In these cases we get so-called *pomerons*, which are color singlet states that do not exchange color between the protons. These interaction processes at high-p_T proton-proton collisions are normally not interesting, since they will produce particles with low transverse momentum close to the beam line. They are then difficult to detect. They are still important for luminosity measurements since they contribute to the total p-p cross-section. These events are detected in special experiments that use *minimum bias* events, where the final state has no requirements or special triggers.

3.2.1 Hard Scattering Events

The more interesting events to look at in high-p_T p-p collisions, are the non-diffraction events. With non-diffractive events, there is an exchange of color between the partons in the interaction. These are called hard scattering events. Hard scattering events with high momentum transfers, Q^2, may create heavy particles. This is the main interest in particle colliders.

A hard scattering event can be expressed as

$$A + B \to c + X, \tag{3.14}$$

where the collision between the partons are expressed as

$$a + b \to c. \tag{3.15}$$

A and B are the two colliding protons, and a and b are the corresponding colliding partons. c are the interesting high p_T objects. X are underlying products which are mostly remnants after the original collision.

In Figure 3.2 we see how a hard scattering p-p collision may look like, with outgoing partons, underlying events, initial- and final-state radiation. The initial-state radiation is mean radiation of gluons or photons from partons before the hard scattering. Final-state radiation is then the mean radiation from the produced partons after the hard interaction. The underlaying events are the further interactions between partons beyond the hard scattering. These interactions will often go out of reach of the detector. Leading to another reason for why we look at the transverse momentum.

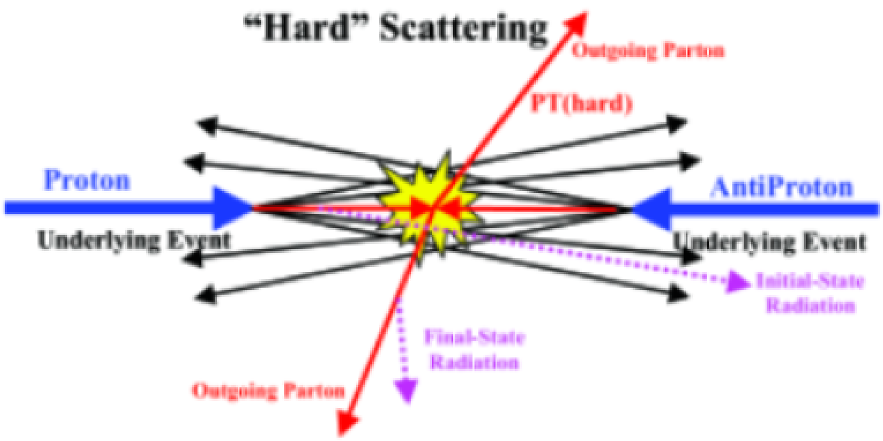

Figure 3.2: Illustration of a hard scattering proton-proton collision. Figure is taken from ref. [37].

3.2.2 Parton Distribution Function

The parton distribution function (PDF)[9] is used to describe the probability density of the two partons, a in proton A and b in proton B, to carry the proton momentum fractions x_a and x_b. These PDFs are also dependent on the squared of the momentum scale indicating the total four-momentum transfer in the collisions Q^2 as $F_{a/A}(x_a, Q^2)$ and $F_{b/B}(x_b, Q^2)$. These PDFs must be found experimentally in Deep Inelastic Scattering (DIS) experiments of leptons against hadrons, since they cannot be calculated from QCD theory. The PDFs are also used to get the cross-section of the collisions.

With the measured PDFs $f(x, Q^2)$, a structure function $F_2^{ep}(x, Q^2)$ can be determined

$$F_2^{ep}(x, Q^2) = 2xF_1^{ep}(x, Q^2) = x \sum_i Q_i^2 f_i(x), \tag{3.16}$$

where i is a quark in the proton and Q_i is the charge of the quark. The interesting here are the $f(x)$ of each of the partons. So results of measurements from several DIS experiments of varying structure functions, which are superpositions of the same $f_i(x)$'s, are combined to get the $f(x)$ for each parton.

3.2.3 Hadronization

We already have covered that quarks and gluons carry color charge (sect. 1.1), and that they are not observed as free particles[10]. They can only be found in colorless objects like hadrons.

We also talked about the strong force, which increases in strength when increasing the distance between (elementary) particles. So if we separate a quark from a hadron, the color field will increase. The quarks the emits gluons, which then becomes new quark-anitquark pairs or gluons, hence making new colored particles. They will then be observed jets of colorless particles. As this production of partons continue, the energy will decrease until it is low enough to produce hadrons. This process of high-energy quarks (and gluons) that produce new jets until we get hadrons, is called *hadronization*. The jets can also be called hadronic showers, since many hadrons are usually produced in hadronization processes.

These jets are not only produced in p-p collisions with hard scattering, but also in the underlying events and initial- and final-state radiation gluons

[9] See chapter 8 in Thomson [1] for more in depth explanations.

[10] Only exception is the top quark with shorter lifetime than the QCD interaction time scale.

in this hard scattering. This makes p-p collisions very complicated and messy when trying to study them, compared to electron-positron collisions.

Chapter 4

Particle Accelerators and Collider Experiments

To fully understand the physics of the particles around us and what things are made of, we need some way of looking at the subatomic world. This is done in huge particle accelerators where particles are accelerated to high velocities and energies, and collided with each other to make other particles. Here the aftermath of the collisions result in new particles with new energies that are detected as they move through detectors.

There are various accelerators and detectors that produce and accelerate different particles in the world. In this chapter we will look at the biggest particle physics laboratory in the world, namely the European Organization for Nuclear Research (CERN[11]), and some of its components like particle accelerators, collisions and detectors.

4.1 CERN

The CERN laboratory lies near Geneva, on the border between France and Switzerland, and was founded in 1954 [38]. It is a multinational collaboration between 23 (mostly) European countries. They also have several international relations with other countries both inside and outside of Europa. CERNs main involvement today is regarding particle physics and particle accelerator experiments. Many of the biggest discoveries in particle physics today, have come from particle experiments at CERN. This includes among others, the discovery of the Higgs boson and discovery of the W and Z bosons. At the main site of CERN in Meyrin, there is also a computer facility that

[11]The name CERN is originally from French; Conseil Européen pour la Recherche Nucléaire.

is used for storing and analyzing data. These data also include simulations of particle and event experiments at CERN. CERN is also the place where Tim Berners-Lee invented the World Wide Web in the late 1980s [39].

CERN consists of several particle accelerators, experiments and facilities in different shapes and sizes. The two main types of accelerators are linear and circular. They are located at various sites, and they accelerate particles to high energies before they are sent to experiments that collides particles with other accelerated particles or particles with stationary targets, or are sent to more powerful accelerators. They are built differently to accelerate different kinds of particles with different masses. In Figure 4.1 we see the CERN accelerator complex. Some of the accelerators are mostly used to pre-accelerate the particles before they are sent to another accelerator where they are accelerated even more. This repeats until the particles reach the desired energy to collide with at one of the detectors. It normally takes about 20 minutes to reach the desired energy.

For the more important discoveries, like the ones we have mentioned above, the W and Z bosons were discovered by the Super Proton Synchrotron (SPS) in 1983. The SPS delivered an energy between 300-450 GeV. It was then later used to accelerate high energy electrons and positrons into the Large Electron-Positron Collider (LEP). LEP is the largest and most powerful lepton collider built to this date, and was most functional between 1989 and 2000. LEP was then replaced by the Large Hadron Collider (LHC) in 2008 to collide protons and heavy ions. We will look more into the LHC later (sect. 4.2).

There are also many plans for the future regarding both upgrades to existing accelerators and building new ones. The two biggest projects is the Compact Linear Collider (CLIC), which is a linear electron-positron collider at higher energies, and the Future Circular Collider (FCC), which is a even larger version of the LHC. This does not only apply at CERN, but several other places in the world like in China (CEPC [41] [42]) and Japan (ILC [43][44]).

4.1.1 Accelerators

As mentioned, there are two main types of accelerators. That is linear and circular accelerators. The first particle accelerators used static high voltage to accelerate charged particles. These accelerators are most suited for lower energies in the MV range depending on the machine. The two main types are the Cockcroft-Walton accelerator and the Van de Graaff accelerator, and they are both linear accelerators.

The more commonly used today is electrodynamic acceleration to give the

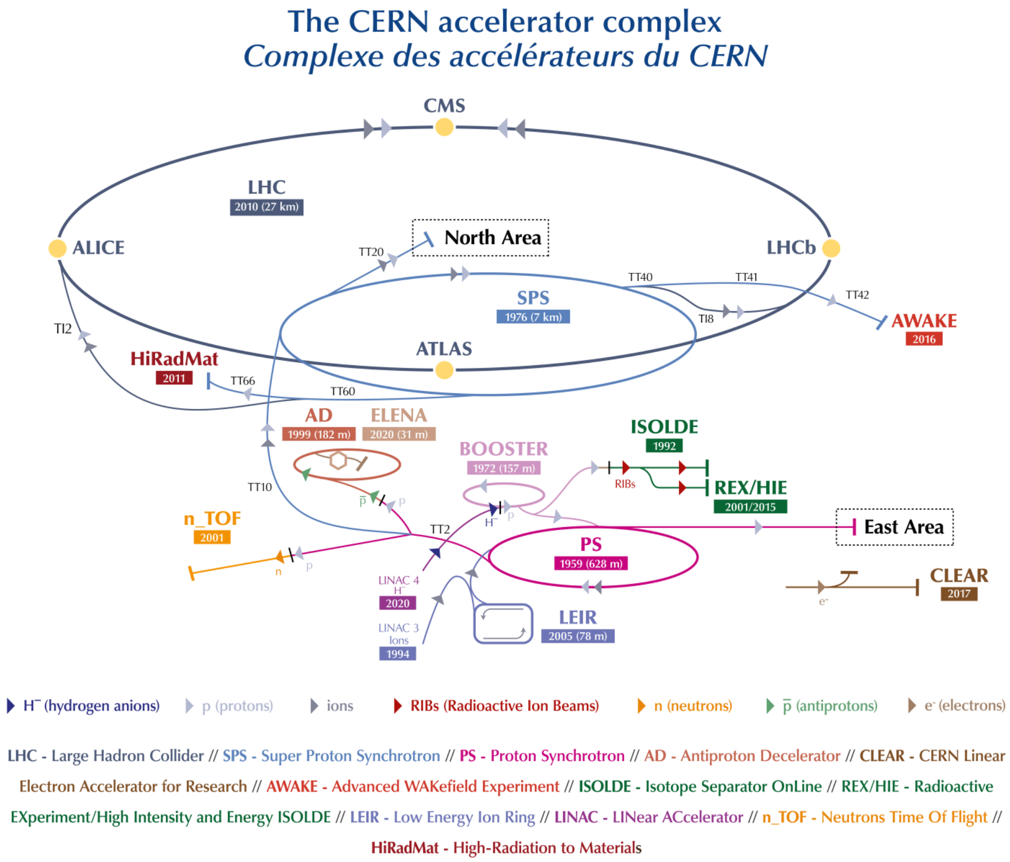

Figure 4.1: The CERN accelerator complex as of 2019. Credit: CERN[40].

particles more energy, either by non-resonant magnetic induction/resonant circuits or cavities filled with oscillating radio frequency (RF) fields. These accelerators give the particles much higher energies than the electrostatic, because of the high voltage ceiling from electric discharge when using the electrostatic.

Linear accelerators

The linear accelerators (linac) consist of several drift tubes that accelerate the particles that passes through them. The drift tubes uses an alternating high-energy field that switch between attracting the particles and then pushing them with increased velocity on the other side. These particles can reach velocities near the speed of light, depending on their initial masses. Most of the linacs are more effective for accelerating electrons and positrons since their masses are so low. The linacs are also very useful for a quick raise in the energy of the particles before injecting them into circular accelerators.

There are also linear induction accelerators that uses increasing magnetic fields due to magnetic induction to accelerate particles. This happens in non-resonant induction cavities that uses a voltage pulse to increase the magnetic field. These accelerators can reach very high beam currents in short pulses.

Circular accelerators

To reach very high beam energies in linacs, they have to be very long. This is not as big of a problem with circular accelerators. With circular accelerators, the particles just move in circles and continue to accelerate until they reach the desired energy for the experiment. This makes the space needed with higher power not as big as for the same power with a linac. To bend the path of the particle beams, electromagnets are used. The disadvantage is that every charged particle emits electromagnetic radiation when accelerated. And when a charged particle is bent around in a circle with magnets, it will emit what is called synchrotron radiation tangent to the circle. The amount of synchrotron radiation that is emitted depends heavily on the masses of the particles.

There are several types of circular accelerators with various differences. One type is the **cyclotron**, which uses a constant uniform magnetic field in a circle with the form of two D-cavities placed opposite of each other, forming a circle construction with an electric field in the gap between. There the accelerated particle moves further and further outwards as the velocity increases from the electric field. To reach higher energies than 15 MeV, the frequency of the electric charge is adjusted to the applied voltage. Now the previously continuous beam is bunched up instead. This accelerator is called the **synchrocyclotron**. This gave a low beam intensity and needed a huge magnet radius for high energies. Next step was to keep the frequency constant and increase the magnetic field. This was the **isochronous cyclotron**, which could have continuous beams with higher intensity. This also needed bigger structures and magnets. To reach even higher energies, the **synchrotron** was introduced. This structure uses a constant radius ring where the magnetic field increases as the particles are accelerated. They need particle beam bunches to be accelerated in cavities cyclically, and uses many hundreds of bending magnets with various functions along the ring.

Some also uses what is called **storage rings**, which is a ring with many magnets with a constant magnetic field where the particle bunches continue their orbit for longer periods of time for closer study or further acceleration.

4.1.2 Colliders

As with the particle accelerators, colliders may be linear or circular. After the particle beams have been accelerated, they are either collided with other particle beams or shot against stationary targets. When the particle beams hit stationary targets, the built up energies is effectively wasted and they simply move the particles in the target. When the beams collide with each other with enough energy, they may produce new particles that often quickly decay into other particles again. These products are what scientists want to study with detectors to get more insight into physics. With colliding particles, the collision energies of the beams that can be reached are much higher than hitting stationary targets since both beams will add to the total energy when colliding. Since the particles are very small, beams at the collision points have to be extremely accurate to being able to hit the desired targets. Storage rings are quite useful for particle collisions when the particle bunches have reached their desired energies. Since the particles might miss each other on the first go, since they are so small, they can go around the ring until they finally collide without loosing to much energy.

4.2 The LHC and Accelerator Experiments

The largest and most powerful (circular/synchrotron) particle accelerator and collider today is the Large Hadron Collider (LHC) [45], which we easily can see in Figure 4.1 as the biggest gray circle around the North Area. The particles are sent in bunches up to 10^{11} particles and are accelerated mostly using radio frequency cavities in a 27 km ring consisting of superconducting magnets, where the particles are boosted in several structures along the ring to the desired energies. The LHC is designed to have 2808 bunches at the same time traveling in the ring. The ring lies 100 m underground in a tunnel beneath the French-Swiss border. Along the ring, there are 4 main crossing points (ATLAS, CMS, ALICE, LHCb) which are detectors that register the particle collisions and the following particle decays. At these collision points, the total collision energy, or center-of-mass energy $\sqrt{s}$, can reach 13 TeV[12]. There are in total seven detectors along the ring, each designed for different experiments.

The first time, run 1, it was used for proton-proton (hadron) collisions in 2010, it reached a record high energy of 3.5 TeV per beam. After upgrades, run 2, it reached an even higher energy of 6.5 TeV per beam. It is currently stopped for another upgrade, which started in 2008. The accelerator sends two high-energy beams, in separate tubes and directions, near the speed of light before they collide at one of the detectors. To reach these high energies, the particle beams are accelerated in several systems that boosts the energies higher and higher before injected into the main LHC ring [46]. Inside the tubes, there is an ultrahigh vacuum. To make sure that the particles are directed correctly through the ring, superconducting electromagnets are used to bend the particle trajectories and keep them inside the ring. The magnets vary in strengths and sizes to direct the beams properly. Since the particles are incredibly tiny, the precision of the magnets have to be extremely good to make the particles hit each other at the collision points. That is also why beams are accelerated and not single particles at a time, and since the construction of the accelerator is a ring they can continue around again when some of them do not collide (remember storage rings sect.4.1.1). A beam can typically go around in the ring for about 10 hours before the beam has lost too much intensity.

As mentioned earlier, there are seven detector experiments at the LHC [47]. The four main, and biggest, detectors in the LHC, have different objectives. The ATLAS and CMS experiments are two large and similar general-purpose particle detectors that looks for new physics and more precise study of the Higgs boson. The ALICE and LHCb experiments have more specific roles, and study the quark-gluon plasma from heavy ion collisions and missing antimatter connected to CP-violation after the Big Bang, respectively. The remaining detectors are much smaller and are used in more specialized research. We will look more at ATLAS and the detector equipment later (sect.4.4).

The LHC is used to explore many different open questions in physics,

[12] The LHC is theorized to a limit of 14 TeV.

like further study of the SM and theories beyond it. In addition to proton-proton collisions, the LHC can also study heavy ion collisions at some of the detectors.

4.2.1 Important Parameters

One of the most important parameters of measurements at particle accelerators, are the center-of-mass energy $\sqrt{s}$ we already have mentioned. For two particles colliding, the Lorentz invariant quantity s (the squared invariant mass) is formed as

$$s = \left(\sum_{i=1}^{2} E_i \right)^2 - \left(\sum_{i=1}^{2} \mathbf{p}_i \right)^2 . \tag{4.1}$$

There are also other important parameters used to describe the performance of particle colliders:

Luminosity

The second most important parameter in particle collider performance is the *luminosity*, $\mathcal{L}$. The design luminosity of the LHC is $\mathcal{L} = 10^{34}$ cm^{-2}s^{-1}. The bunches at the LHC are separated by 25 ns, which corresponds to a frequency of $f = 40$ MHz. The (instantaneous) luminosity is used to describe the number of collisions per area per second as[13]

$$\mathcal{L} = f \frac{n_1 n_2}{4\pi\sigma_x\sigma_y}, \tag{4.2}$$

where f is the frequency of the particle beam bunches colliding (bunch crossing rate), n_1 and n_2 are the number of particles in the colliding bunches and σ_x and σ_y are the root-mean-square (rms) horizontal and vertical beam sizes.

The complete collider luminosity at the LHC can be written in terms of colliding beam parameters [48]

$$\mathcal{L} = f \frac{n_1 n_2 n_b}{4\pi\sigma_x\sigma_y} F(\sigma_x, \sigma_y, \sigma_s, \Phi). \tag{4.3}$$

This equation has the same parameters as in equation 4.2, except for two additional parameters. n_b is the number of proton bunches. F is a geometrical reduction factor accounting for the non-zero-crossing angle at the interaction point, depending on the two rms beam sizes, the beam length σ_s and the crossing angle Φ.

[13]With the assumption of Gaussian profile beams and head-on collisions.

Rate

After calculating the cross-section, σ, of a collision process, the (event) *rate*, R, after accumulating many such collisions, is calculated as

$$R = \sigma \mathcal{L}. \tag{4.4}$$

Number of interactions

The total number of expected events of particles collisions over a given time, is the time integration of the event rate

$$N = \sigma \int \mathcal{L} dt. \tag{4.5}$$

The time-integral of the luminosity, $\int \mathcal{L} dt$, is often called the *integrated luminosity*, and is given in inverse femtobarns $[fb^{-1}]$.

Cross-section

Precise measurements of properties like transverse profiles are hard to get exact. This means that the instantaneous luminosity is difficult to measure accurately. Cross-section measurements are then made with reference to a process with already known cross-section, σ_{ref}. The measured cross-section is then calculated as

$$\sigma = \sigma_{\text{ref}} \frac{N}{N_{\text{ref}}}, \tag{4.6}$$

where N is the counted number of interesting events and N_{ref} is the number of observed events for the reference process.

The cross-section for p-p collisions at the LHC for $\sqrt{s} = 13$ TeV measured by the ATLAS experiment to be $\sigma \approx 78$ mb [49].

Pile-up

In particle collisions, we want a high instantaneous luminosity. This means that the intensity of the proton beam need to be high. But with high intensity proton beams, the probability of having more than one proton undergoing an inelastic interaction per bunch crossing is increased. This leads to what is called *pile-up* events, where there are several collisions from the same bunch crossing. This means we need very accurate measurements in detection of the particle tracks to distinguish which new particles comes from which collisions. The main event that is normally used in detection, and this corresponding vertex is called the *primary vertex*.

So since we want higher and higher luminosity to get more collisions, we also get more pile-ups. This need to be controlled to being able to use the data we get from the detectors of the collisions. The additional collisions do luckily normally have very small momentum transfers, which means we can characterize them as minimum bias events.

4.3 Interactions of Particles with Matter

To detect the particles produced in particle colliders like the LHC, the particles have to interact with matter in the detectors. The particles also need to be stable and live long enough to be detected. Only the electron, proton, photon and neutrinos are considered stable of the known elementary particles. The unstable particles doe not decay until they have traveled a distance of order $\gamma v \tau$, where γ is the already known Lorentz factor (relativistic time dilatation) and τ is the mean lifetime of the particle in its rest frame. When the relativistic particle lifetimes are longer than 10^{-10}s, they will normally live long enough to be detected. Heavier particles has generally a shorter lifetime than lighter particles.

The particle interactions can be categorized into three categorizes: i) interactions between charged particles, ii) electromagnetic interactions between electrons and photons and iii) strong interactions of charged and neutral hadrons.

This section is based upon chapter 1.2 in Thomson [1].

4.3.1 Charged Particles

Ionization

Every electrically charged particle will interact electromagnetically. A relativistic charged particle will interact with the atomic electrons and lose energy through ionization of the atoms when it passes through a medium. This energy loss per unit length traversed through the medium by a single charged particle with velocity $v = \beta c$ is given by the Bethe-Bloch equation

$$\frac{dE}{dx} \approx -4\pi\hbar^2 c^2 \alpha^2 \frac{nZ}{m_e v^2}\left[\ln\left(\frac{2\beta^2\gamma^2 c^2 m_e}{I_e}\right) - \beta^2\right], \tag{4.7}$$

where α is a fine-structure constant, Z is the atomic number of the medium, n is the number density of the atoms in the medium and $I_3 \sim 10Z$ eV is the effective ionization of the material averaged over all atomic electrons. From this Bethe-Bloch equation, we see that it is largest when the velocity is low.

For particle colliders, we are more interested in highly relativistic particles, $v \approx c$. In this case, dE/dx will depend logarithmically on $\beta^2\gamma^2$, where

$$\beta\gamma = \frac{v/c}{\sqrt{1-(v/c)^2}} = \frac{p}{mc} \tag{4.8}$$

makes the rate of ionization energy loss slowly rise as this factor (and p) increases. The ionization energy loss when considering the material, does not depend significantly on the material except for the material density ρ.

The energy loss due to this ionization is small, making particles where ionization is the main mechanism of energy loss able to travel long distances before their energy is completely lost. The importance of ionization differs for different type of particles. The track of ionized atoms behind charged particles that traverse through media, is used to track the trajectory of the particles.

4.3.2 Electrons and Photons

Bremsstrahlung

Another way for charged particles to lose energy, is when the energies become higher than a certain "critical energy"

$$E_c \sim \frac{800}{Z}\mathrm{MeV} \tag{4.9}$$

related to the charge Z of the nucleus. Then the electrons will radiate a photon in the electrostatic field of a nucleus. This process of energy loss is called bremsstrahlung. For lower energies, ionization will dominate the energy loss. This process can happen for all charged particles, since the rate is proportional to the square of the mass of the particle. So as long as the energy of the particle becomes high enough, the bremsstrahlung process will have a bigger and bigger effect on the energy loss rate. This is most interesting with electrons since they get energies in the several GeV order ranges in particle experiments, way above the critical energy yielding primarily rate of energy loss due to bremsstrahlung. The typical order of the critical energy of electrons are in the order of a few tens of MeV. In lead, the critical energy for electrons are approximately $E_c \sim 10$ MeV.

The average distance over which the energy of an electron is reduced by bremsstrahlung by a factor of $1/e$, is called the *radiation length* X_0, and is dependent on the classical radius of an electron

$$r_e = \frac{e^2}{4\pi\epsilon_0 m_e c^2} = 2.8 \times 10^{-15}\ \mathrm{m}. \tag{4.10}$$

Photoelectric effect

Photons will primarily interact with materials by the photoelectric effect at low energies. The photon is then absorbed by an atomic electron which is ejected from the atom.

When the energy is around $E_\gamma \sim 1$ MeV, the Compton scattering process will dominate the process. When the photon interacts with an atomic electron here, the photon will be inelastically scattered and lose some of its energy to the electron.

At higher energies around $E_\gamma > 100$ MeV, the electron-positron pair production will dominate the process through photon interaction with the electromagnetic field of the atomic nucleus.

Electromagnetic shower

When the energy of the an electron is high enough that it radiates a bremsstrahlung photon when it interacts with a medium, the photon will produce a e^+e^- (electron-positron) pair. These new photons, electrons and positrons continue to interact with the medium and continue to produce new particles. This process is called an electromagnetic shower. This also happens when the energy of a photon is high enough.

The number of particles in an electromagnetic shower approximately doubles after every radiation length of material traversed. An illustration of an electromagnetic shower starting with an electron can be seen in Figure 4.2. The average energy of individual particles after x radiation lengths of an electromagnetic shower produced by an electron or photon is

$$\langle E \rangle \approx \frac{E}{2^x}. \tag{4.11}$$

The shower will continue to develop until the average energy goes below the critical energy E_c (eq. 4.9). From then on, the energy loss of the electrons and photons comes from ionization. There is then a maximum number of particles after x_{max} radiation lengths, at $\langle E \rangle = E_c$. The maximum radiation length is then

$$r_{max} = \frac{\ln(E/E_c)}{\ln 2}. \tag{4.12}$$

Electromagnetic showers will deposit most of their energy in a relatively small region of space. Most electromagnetic showers will also have more or less the same energy, since they will have a large number of particles leading to small fluctuations of different electromagnetic showers.

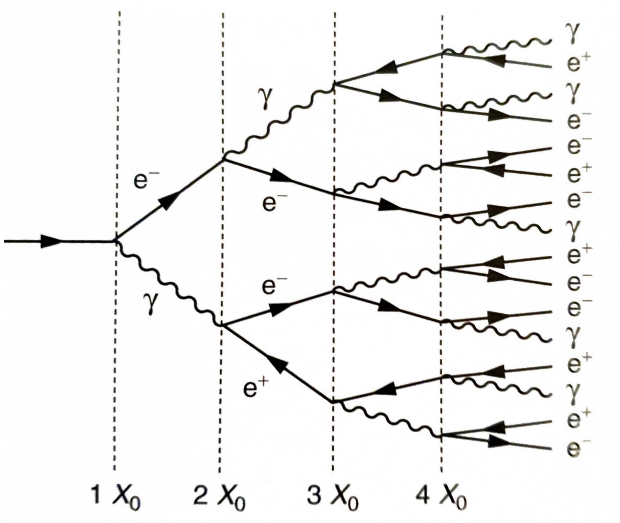

Figure 4.2: Illustration of an electromagnetic shower, beginning with an electron. Credit: ref. [1].

4.3.3 Hadrons

Like charged leptons, charged hadrons will lose energy by ionization as they traverse matter. Charged and neutral hadrons can also interact through the strong interaction by emission of a quark-antiquark pair. These types of hadronic interactions will make the hadrons split and make new hadrons and jets, leading to hadronic showers similar to electromagnetic showers. As we know, hadrons producing jets makes the hadronic shower less uinform than the electromagnetic shower. This comes from that hadronic showers can create more different final-state particles through the strong interaction than electromagnetic showers. The hadronic showers are parametrized by the mean distance between hadronic interactions of relativistic hadrons, which is called the nuclear interaction length λ_I. The nuclear interaction length is analogous to the radiation length, but it is much larger.

The hadronic showers can also get an electromagnetic component from the decay of a neutral pion (π^0) produced in the shower, since it decays almost instantaneously as $\pi^0 \to \gamma\gamma$. The fraction of electromagnetic components depends on how many neutral pions are produced in the hadronic showers. Not all of the energy in a hadronic shower many not be detected. Only on average 30% of incident energy is lost from nuclear excitation and break-up.

4.4 The ATLAS Experiment and Particle Detection

To detect the particles produced at particle colliders, we need different instruments that can detect the various types of particle interactions we have looked at in the last section. The largest detector at the LHC is the ATLAS (A Toroidal LHC ApparatuS) experiment. The ATLAS detector is 25 m in diameter, 46 m long and weights about 7000 tons. The cylindrical shape of ATLAS is optimized to detect as many particles as possible, and covers almost a 4π angle with detectors. Like we mentioned earlier for particle collisions in the LHC, the ATLAS also uses the same Cartesian coordinate system with the z-direction as the direction of the beams, y-direction is upwards and x-direction is towards the center of the accelerator circle. It also uses a spherical coordinate system with the azimuthal angle ϕ in the xy-plane around the beam axis, and the polar angle θ is the angle from the beam axis. To measure the distance between the particles, the angular distance ΔR (eq.3.12) in the $\phi\eta$-plane.

The detector can be divided into three parts; the central part is defined where the pseudo-rapidity is $|\eta| \lesssim 2.0$ and is called the *barrel*, and the two end parts ($|\eta| \gtrsim 2.0$) are called *end-caps*. In Figure 4.3 we see a computer generated image of the ATLAS detector with pointers to the main components.

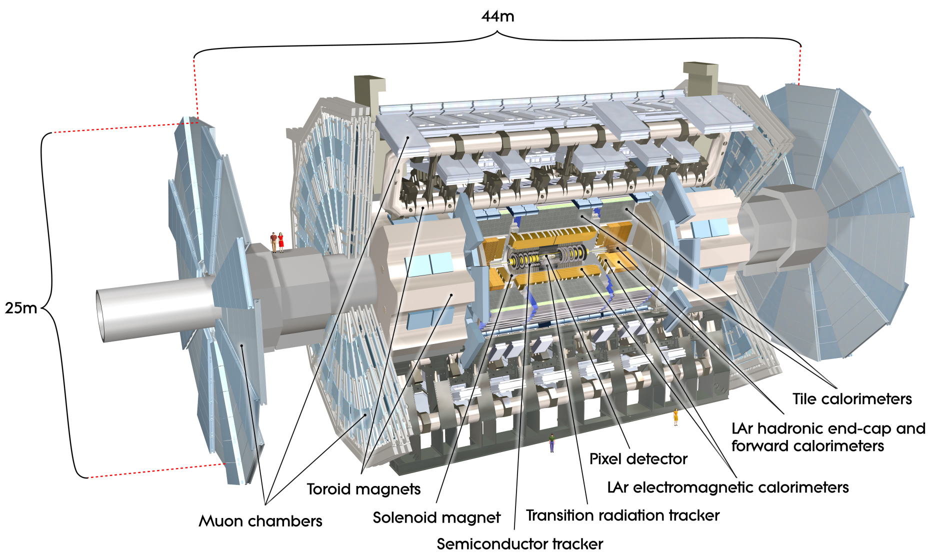

Figure 4.3: The ATLAS detector. Credit: ref. [50].

The ATLAS detectors is designed to be a general-purpose detector, covering a wide range of signals. Some of the many particle properties the ATLAS detector can detect is the mass, momentum and energies of the particles. For ATLAS to detect these properties, it has a layered design of detectors that is designed to observe specific properties of the particles. These detectors use the various particle traces to identify and measure the properties of the particles. The ATLAS detector consists of five main systems; the inner detector (ID), different calorimeters, a muon spectrometer (MS), a magnet system and a trigger and data system. The main systems also consists of smaller sub-systems, which we will take a brief look at next. In Figure 4.4, we see a sketch of the detector layout systems and how some particles behave in these different tracking systems.

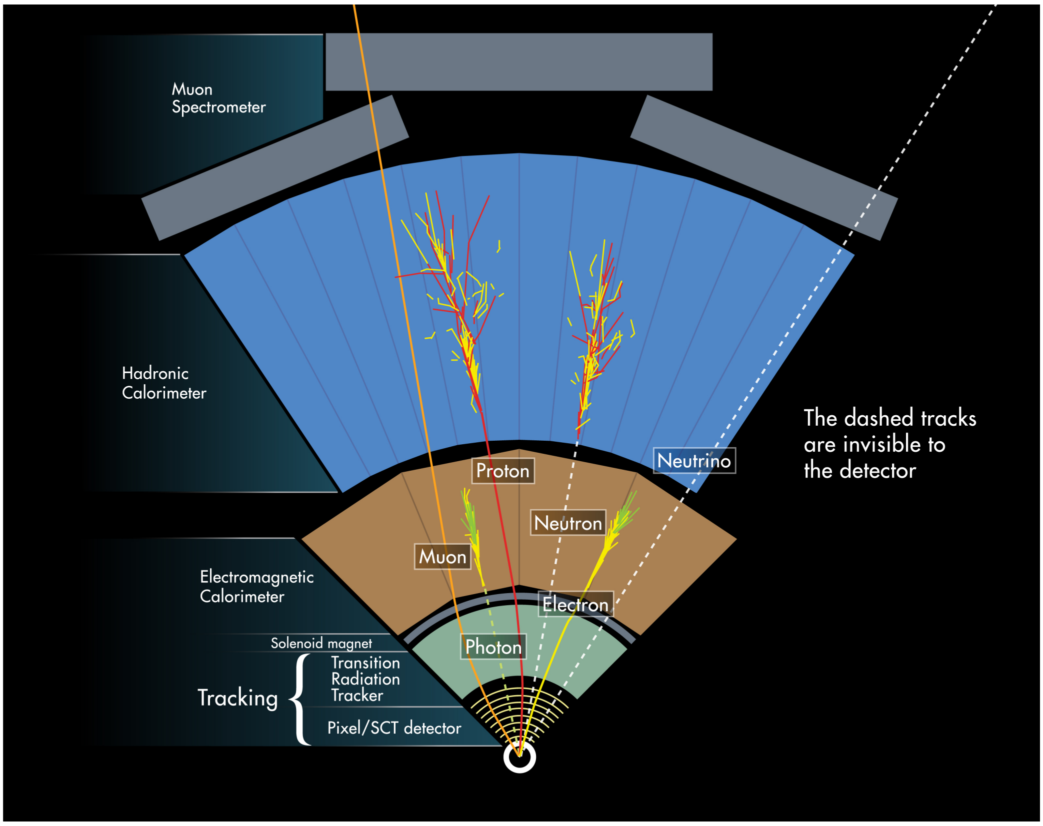

Figure 4.4: An illustration of the main tracking systems in the ATLAS detector, including how some particles behave in the various systems. Credit: ref. [51].

4.4.1 Inner Detector

The inner detector tracks charged particles that leaves traces of ionized atoms when traveling through a medium. The tracks, momentums and charges of the particles can be traced in a 2 T magnetic field that makes the charged particles curve. The degree of the curvature is used to determined the charge and the momentum.

The inner detector consists of three sub-systems. The most inner part is a silicon Pixel Detector that is used for extremely precise tracking near the interaction point of the particle collisions, which covers $|\eta| < 2.5$. The second part is a Semiconductor Tracker (SCT) that covers a bigger area than the pixel detector for the particle tracking and uses longer and narrow strips instead of pixels. The SCT provides detection in the range of $|\eta| < 2.5$ as well. The third part is a Transition Radiation Tracker (TRT) that covers an even larger area with lower spatial resolution, and can detect transition radiation photons by using gas filled drift/straw tubes. The TRT provides the capability of electron identification for a variety of energies since the transition radiation gives out a stronger signal than ionization signal. It has a coverage of $|\eta| < 2$.

4.4.2 Calorimeters

Outside the ID and the solenoid magnet system, there follows two types of calorimeters; an inner electromagnetic calorimeter and an outer hadronic calorimeter. Their purpose is to measure the energy of the passing particles and particle showers especially. They both consist of a barrel part and two end-cap parts.

The **electromagnetic** calorimeter (ECal) measures particles that interact electromagnetically like charged particles and photons. The ECal is made of layers of lead absorbing plates and liquid argon, and covers the whole ϕ angle around the beam axis. The energy is measured in the liquid argon, and free electrons are picked up by electrodes. The ECal is covered by cryostats to keep it at the correct low temperature. The thickness of the ECal is measured in radiation lengths X_0, which is the mean length required to reduce the energy of a particle by $1/E$ in a material. The thickness of the barrel part is $\geq 22X_0$, while the end-caps are $\geq 24X_0$.

The **hadronic** calorimeter (HCal) measures hadrons and hadronic showers[14]. The HCal is made of several layers of steel absorbers and plastic scintillator tiles that alternates. The HCal is a lot bigger than the ECal, since the

[14]It measures the energy of particles that interact via the strong force, which is mainly hadrons.

distance between nuclear interactions are relatively large. The HCal consists of three parts where two of them share some of the same parts as the ECal. The iron in the detector both slows down and traps hadrons and functions as a bending magnet used to reveal the charge and identity of the particles. The HCal is not as precise as the ECal. The thickness of the HCal is measured in interaction lengths λ, which is the mean distance a particle travels before interacting strongly with the material. The detector is 9.7 interaction lengths thick [52].

4.4.3 Muon Spectrometer

Outside the calorimeters, we find the muon spectrometer. Here high-energy muons are detected. Only the neutrinos should now go undetected through the detectors, in principle, and they are normally identified as missing momentum or *MET*. This comes from the energy conservation law, where the sum of the measured momenta of the all particles produced should be zero. This detector is very large, 11 m radius [53], and consist of three parts as well as a barrel and two end-caps; a magnetic field with three toroidal magnets, a set of 1200 chambers which measure the tracks of the muons and a set of triggering chambers with accurate time-resolution. The detection of the muons happen the same way as before, by measuring their momentum as they are bent in the detector. They should also be simpler to identify since all other identifiable particles should not reach this far out from the interaction point.

4.4.4 Magnet System

ATLAS uses two types of superconducting magnet systems to measure the momentum from the bending of the particles through the Lorentz force. The magnet system consists of a central solenoid, a barrel toroid and two end-cap toroids. The central solenoid is located between the inner detector and the electromagnetic calorimeter, which produces the 2 T magnetic field for the ID. The barrel toroid produces a magnetic field of 0.5 T, and is located around the middle cylinder of the MS barrel outside the calorimeters. The two end-cap toroids produce magnetic fields of 1 T, and located at the end-cap regions of the Muon System.

4.4.5 Trigger System

The detector produces a huge amount of data, which need to be stored and processed. The output event storage rate have to be reduced from an initial bunch crossing of 40 MHz to ~200 Hz . To only get the most interesting data for further analysis, a trigger system is used to extract these relevant events. The ATLAS Trigger and Data Acquisition system (TDAQ) has three levels for reducing the amount of stored data [54]; the Level 1 (LVL1) trigger is hardware-based and makes quick decisions of which events to store, the Level 2 (LVL2) and the Event filters (EF) are software-based and are often combined to and referred to as the High Level Triggers (HLT). Only the events passing both the LVL1 and HLT are stored for further analysis.

The LVL1 trigger uses information from the calorimeters and the muon spectrometer to choose the events with high p_T particles, large MET (E_T^{miss}) events and large total transverse energy E_T events. These events are then classified as interesting as passed on to the next trigger. The LVL1 trigger also defines regions based on the ϕ and η coordinates from the interesting events.

The LVL2 trigger uses all the information within the regions of interest (ROIs) defined by the LVL1 trigger to further reduce the amount of event data. The accepted events are then assembled put together into a full event. The EF uses an offline analysis to even further reduce the data used to store and further analysis at the CERN Computer Center.

Chapter 5

The Charge Current Drell-Yan Process

Our model is based on the works of Das et al. [28], Pascoli et al. [27] and CMS Collaboration et al. [55] with a $SU(2)_L \times SU(2)_R \times U(1)_{B-L}$ gauge theory combined with the inverse seesaw mechanism, where two protons are accelerated and collided to produce a heavy $W_R^{\pm}$ boson and a left-right symmetric model. Since the inverse seesaw mechanism allows large left-right neutrino mixing while keeping the neutrino masses tiny, the W_R boson may decay into a charged lepton l and a heavy pseudo-Dirac neutrino N. The pseudo-Dirac neutrino then decays into another lepton and another W_R boson with opposite sign, which then decays into another lepton and missing transverse energy (MET)/a (light) neutrino:

$$q\bar{q} \to W_R \to l_1 N_l \to l_1 l_2 W_R^* \to l_1 l_2 l_3 \nu$$

The final state is then three charged leptons (trilepton) plus missing transverse energy which goes undetected as a neutrino. This decay process can be seen in Figure 5.1, and is produced through the charged current (CC) Drell-Yan (DY) process [27].

The decay products of such particle collisions can be detected in experiments like the LHC and ATLAS at CERN (sect. 4.4). These events can also be simulated, meaning that we can simulate proton-proton collision events and the decay processes, like at the LHC. For each decay final state product, we can measure many properties like momentum, the transverse momentum, the polar angle and the azimuthal angle. We can also detect what kind of quarks that collide[14], and which final state particles are produced. With these particle properties we can calculate the angles and angular distance

[14] Remember that we effectively collide the quarks in the protons.

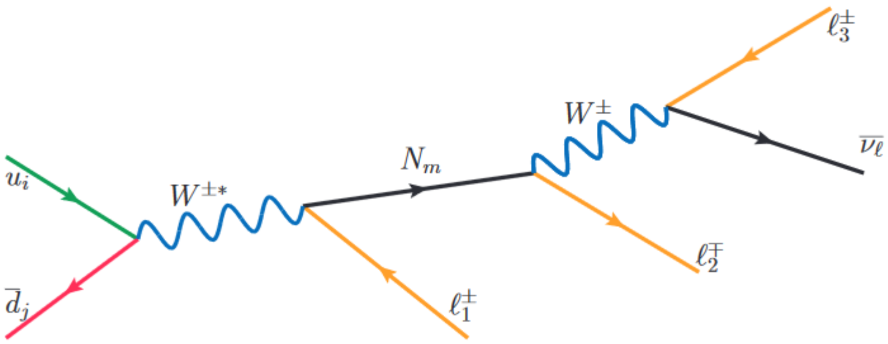

Figure 5.1: The Born diagram for the charged current Drell-Yan process of the proton-proton collision producing a heavy pseudo-Dirac neutrino N in the inverse seesaw mechanism model, leading to a trilepton plus missing transverse energy (a light neutrino) final state. Figure is taken from ref. [27].

between each produced particle and the neutrino. We should then be able to find out which lepton comes from which decay branch in the decay process in Figure 5.1 computationally.

The end goal is then to make a program that can automatically identify each lepton, and where it came from, by using these particle properties by using what is called machine learning. We will look more into what machine learning is in the next chapter.

Chapter 6

Machine Learning

...

Chapter 7

Data/Samples/Machine tools for producing the data?

Chapter 8

The Search/Analysis/Methods?

Chapter 9

Results?

Conclusion

Appendix A

Appendix?

List of Figures

Bibliography

[1] Mark Thomson. *"Modern particle physics*. Cambridge University Press, 2013.

[2] Glenn Elert. The physics hypertextbook, 1998-2020. URL https://physics.info/standard/.

[3] *Why is the Higgs discovery so significant?* Science and Technology Facilities Council, 2017. URL https://stfc.ukri.org/research/particle-physics-and-particle-astrophysics/peter-higgs-a-truly-british-scientist/why-is-the-higgs-discovery-so-significant/.

[4] Benjamin P Abbott, Richard Abbott, TD Abbott, MR Abernathy, Fausto Acernese, Kendall Ackley, Carl Adams, Thomas Adams, Paolo Addesso, RX Adhikari, et al. Observation of gravitational waves from a binary black hole merger. *Physical review letters*, 116(6):061102, 2016.

[5] Georges Aad, Tatevik Abajyan, B Abbott, J Abdallah, S Abdel Khalek, Ahmed Ali Abdelalim, R Aben, B Abi, M Abolins, OS AbouZeid, et al. Observation of a new particle in the search for the standard model higgs boson with the atlas detector at the lhc. *Physics Letters B*, 716(1):1–29, 2012.

[6] Serguei Chatrchyan, Vardan Khachatryan, Albert M Sirunyan, Armen Tumasyan, Wolfgang Adam, Ernest Aguilo, Thomas Bergauer, M Dragicevic, J Erö, C Fabjan, et al. Observation of a new boson at a mass of 125 gev with the cms experiment at the lhc. *Physics Letters B*, 716(1): 30–61, 2012.

[7] Michela Massimi. *Pauli's Exclusion Principle*. Cambridge University Press, 2005. ISBN 0-521-83911-4.

[8] Y Fukuda, T Hayakawa, E Ichihara, K Inoue, K Ishihara, Hirokazu Ishino, Y Itow, T Kajita, J Kameda, S Kasuga, et al. Evidence for

oscillation of atmospheric neutrinos. *Physical Review Letters*, 81(8): 1562, 1998.

[9] Elizabeth Gibney and Davide Castelvecchi. Neutrino flip wins physics prize, 2015.

[10] Alan Kostelecky. The status of cpt. *arXiv preprint hep-ph/9810365*, 1998.

[11] Franz Mandl and Graham Shaw. *Quantum field theory*. John Wiley & Sons, 2010.

[12] M. Bellac. Quantum and statistical field theory. 1991.

[13] Richard P Feynman. The principle of least action in quantum mechanics. In *Feynman's Thesis—A New Approach To Quantum Theory*, pages 1–69. World Scientific, 2005. doi: https://doi.org/10.1142/9789812567635_0001.

[14] Gerhard Ecker. Quantum chromodynamics. *arXiv preprint hep-ph/0604165*, 2006.

[15] C. N. Yang and R. L. Mills. Conservation of isotopic spin and isotopic gauge invariance. *Phys. Rev.*, 96:191–195, Oct 1954. doi: 10.1103/PhysRev.96.191. URL https://link.aps.org/doi/10.1103/PhysRev.96.191.

[16] Richard Phillips Feynman. *QED: The strange theory of light and matter*. Princeton University Press, 2006.

[17] Guido Altarelli. The standard electroweak theory and beyond. *arXiv preprint hep-ph/9811456*, pages 27–93, 2000.

[18] Sheldon L Glashow. Partial-symmetries of weak interactions. *Nuclear physics*, 22(4):579–588, 1961. doi: https://doi.org/10.1016/0029-5582(61)90469-2.

[19] Steven Weinberg. A model of leptons. *Physical review letters*, 19(21): 1264, 1967. doi: https://doi.org/10.1103/PhysRevLett.19.1264.

[20] A Salam. N. svartholm, ed. elementary particle physics: Relativistic groups and analyticity. In *Eighth Nobel Symposium. Stockholm: Almquvist and Wiksell*, page 367, 1968.

[21] *Press release: The Nobel Prize in Physics 1979*. Nobel Media AB 2020, 1979. URL https://www.nobelprize.org/prizes/physics/1979/press-release/.

[22] Abdus Salam and Steven Weinberg. Nobel Prize for Physics, 1979. *CERN Courier*, page 395, 1979.

[23] Jeffrey Goldstone. Field theories with «superconductor» solutions. *Il Nuovo Cimento (1955-1965)*, 19(1):154–164, 1961. doi: 10.1007/BF02812722.

[24] Howard Baer and Xerxes Tata. *Weak scale supersymmetry: From superfields to scattering events*. Cambridge University Press, 2006.

[25] STEPHEN P. MARTIN. A supersymmetry primer. *Advanced Series on Directions in High Energy Physics*, page 1–98, Jul 1998. ISSN 1793-1339. doi: 10.1142/9789812839657_0001. URL http://dx.doi.org/10.1142/9789812839657_0001.

[26] Rabindra N Mohapatra. Seesaw mechanism and its implications. In *SEESAW 25*, pages 29–44. World Scientific, 2005.

[27] Silvia Pascoli, Richard Ruiz, and Cedric Weiland. Heavy neutrinos with dynamic jet vetoes: multilepton searches at $\sqrt{s}$= 14, 27, and 100 TeV. *Journal of High Energy Physics*, 2019(6):49, 2019.

[28] Arindam Das, Natsumi Nagata, and Nobuchika Okada. Testing the 2-TeV resonance with trileptons. *Journal of High Energy Physics*, 2016 (3):49, 2016.

[29] Darwin Chang and Otto CW Kong. Pseudo-dirac neutrinos. *Physics Letters B*, 477(4):416–423, 2000.

[30] KRS Balaji, Anna Kalliomäki, and Jukka Maalampi. Revisiting pseudo-dirac neutrinos. *Physics Letters B*, 524(1-2):153–160, 2002.

[31] R. N. Mohapatra and J. C. Pati. "natural" left-right symmetry. *Phys. Rev. D*, 11:2558–2561, May 1975. doi: 10.1103/PhysRevD.11.2558. URL https://link.aps.org/doi/10.1103/PhysRevD.11.2558.

[32] Jogesh C. Pati and Abdus Salam. Lepton number as the fourth "color". *Phys. Rev. D*, 10:275–289, Jul 1974. doi: 10.1103/PhysRevD.10.275. URL https://link.aps.org/doi/10.1103/PhysRevD.10.275.

[33] Rabindra N. Mohapatra and Jogesh C. Pati. Left-right gauge symmetry and an "isoconjugate" model of CP violation. *Phys. Rev. D*, 11:566–571, Feb 1975. doi: 10.1103/PhysRevD.11.566. URL https://link.aps.org/doi/10.1103/PhysRevD.11.566.

[34] G. Senjanovic and R. N. Mohapatra. Exact left-right symmetry and spontaneous violation of parity. *Phys. Rev. D*, 12:1502–1505, Sep 1975. doi: 10.1103/PhysRevD.12.1502. URL https://link.aps.org/doi/10.1103/PhysRevD.12.1502.

[35] PS Bhupal Dev, Rabindra N Mohapatra, Werner Rodejohann, and Xun-Jie Xu. Vacuum structure of the left-right symmetric model. *Journal of High Energy Physics*, 2019(2):154, 2019.

[36] Eirik Gramstad. Searches for Supersymmetry in di-Lepton Final States with the ATLAS Detector at $\sqrt{s}$= 7 TeV. 2013.

[37] Richard D Field. The underlying event in hard scattering processes. *arXiv preprint hep-ph/0201192*, 2002.

[38] About CERN. CERN, (10.12.20). URL https://home.cern/about.

[39] Stephanie Sammartino McPherson. *Tim Berners-Lee: Inventor of the World Wide Web*. Twenty-First Century Books, 2009.

[40] Esma Mobs. The CERN accelerator complex - 2019. Complexe des accélérateurs du CERN - 2019. Jul 2019. URL https://cds.cern.ch/record/2684277. General Photo.

[41] XinChou Lou. The Circular Electron Positron Collider. *Nat. Rhev. Phys.*, 1:232–234, 2019. doi: https://doi.org/10.1038/s42254-019-0047-1.

[42] Jie Gao. China's bid for a circular electron-positron collider. *CERN Courier*, 2018.

[43] Shinichiro Michizono. The International Linear Collider. *Nat. Rhev. Phys.*, 1:244–245, 2019. doi: https://doi.org/10.1038/s42254-019-0044-4.

[44] Philip Bambade, Tim Barklow, Ties Behnke, Mikael Berggren, James Brau, Philip Burrows, Dmitri Denisov, Angeles Faus-Golfe, Brian Foster, Keisuke Fujii, et al. The international linear collider: a global project. *arXiv preprint arXiv:1903.01629*, 2019.

[45] The Large Hadron Collider. CERN, (11.12.20). URL https://home.cern/science/accelerators/large-hadron-collider.

[46] Accelerators. CERN, (11.12.20). URL https://home.cern/science/accelerators.

[47] Experiments: LHC experiments. CERN, (11.12.20). URL https://home.cern/science/experiments.

[48] A Airapetian, V Dodonov, L Micu, D Axen, V Vinogradov, D Akerman, B Szeless, P Chochula, C Geich-Gimbel, P Schacht, et al. *ATLAS detector and physics performance: Technical Design Report, 1*, volume 1. 1999.

[49] ATLAS Collaboration. Measurement of the Inelastic Proton-Proton Cross Section at $\sqrt{s}$=13 TeV with the ATLAS Detector at the LHC. *Phys. Rev. Lett.*, 117:182002, Oct 2016. doi: 10.1103/PhysRevLett.117.182002. URL https://link.aps.org/doi/10.1103/PhysRevLett.117.182002.

[50] Computer generated image of the whole ATLAS detector. CERN Document Server, (01.01.21). URL https://cds.cern.ch/record/1095924?ln=en.

[51] How ATLAS detects particles: diagram of particle paths in the detector . CERN Document Server, (01.01.21). URL https://cds.cern.ch/record/1505342?ln=en.

[52] ATLAS Collaboration, Georges Aad, JM Butterworth, J Thion, U Bratzler, PN Ratoff, RB Nickerson, JM Seixas, I Grabowska-Bold, F Meisel, S Lokwitz, et al. The atlas experiment at the cern large hadron collider. *Jinst*, 3:S08003, 2008.

[53] CERN. Overall detector concept. *ATLAS Technical Proposal*, 1994.

[54] DA Scannicchio. Atlas trigger and data acquisition: Capabilities and commissioning. *Nuclear Instruments and Methods in Physics Research Section A: Accelerators, Spectrometers, Detectors and Associated Equipment*, 617(1-3):306–309, 2010.

[55] CMS Collaboration, Vardan Khachatryan, Albert M Sirunyan, Armen Tumasyan, Wolfgang Adam, Thomas Bergauer, Marko Dragicevic, Janos Erö, Christian Fabjan, Markus Friedl, Rudolf Fruehwirth,

et al. Search for heavy neutrinos and W bosons with right-handed couplings in proton-proton collisions at $\sqrt{s}$= 8TeV. *The European Physical Journal C*, 74(11):3149, 2014. doi: https://doi.org/10.1140/epjc/s10052-014-3149-z.